

Submarine eruption-fed and resedimented pumice-rich facies: the Dogashima Formation (Izu Peninsula, Japan)

Martin Jutzeler · Jocelyn McPhie · Sharon R. Allen

Received: 2 November 2013 / Accepted: 1 August 2014 / Published online: 24 September 2014
© Springer-Verlag Berlin Heidelberg 2014

Abstract In the Izu Peninsula (Japan), the Pliocene pumice-rich Dogashima Formation (4.55 ± 0.87 Ma) displays exceptional preservation of volcanoclastic facies that were erupted and deposited in a below wave-base marine setting. It includes high-concentration density current deposits that contain clasts that were emplaced hot, indicating an eruption-fed origin. The lower part of the Dogashima 2 unit consists of a very thick sequence (<12 m) of massive grey andesite breccia restricted to the base of a submarine channel, gradationally overlain by pumice breccia, which is widespread but much thinner and finer in the overbank setting. These two breccias share similar mineralogy and crystal composition and are considered to be co-magmatic and derived from the destruction of a submarine dome by an explosive, pumice-forming eruption. The two breccias were deposited from a single, explosive eruption-fed, sustained, sea floor-hugging, water-supported, high-concentration density current in which the clasts were sorted according to their density. At the rim of the channel, localised good hydraulic sorting of clasts and stratification in the pumice breccia are interpreted to reflect local current expansion and unsteadiness rather than to be the result of hydraulic sorting of clasts during fall from a submarine eruption column and/or umbrella plume. A bimodal coarse (>1 m) pumice- and ash-

rich bed overlying the breccias may be derived from delayed settling of pyroclasts from suspension. In Dogashima 1 and 2, thick cross- and planar-bedded facies composed of sub-rounded pumice clasts are intercalated with eruption-fed facies, implying inter-eruptive mass-wasting on the flank of a submarine volcano, and reworking and resedimentation by high-energy tractional currents in a below wave-base environment.

Keywords Submarine pumice · High-concentration density current · Hydraulic sorting · Eruption-fed · Resedimented · Dogashima Formation

Introduction

The explosive nature of submarine volcanic activity is clearly evident from uplifted successions (e.g. Fiske and Matsuda 1964; Fiske 1969; Cas and Wright 1991; McPhie et al. 1993; Kano et al. 1994, 1996; Kano 1996, 2003; Allen and McPhie 2000, 2009; Raos and McPhie 2003; White et al. 2003; Stewart and McPhie 2004) and historical eruptions (Reynolds et al. 1980; Fiske et al. 1998; Kano 2003; Rivera et al. 2013; Jutzeler et al. 2014a, b) and can be inferred from the presence of modern calderas on the sea floor (Wright and Gamble 1999; Fiske et al. 2001; Tani et al. 2008; Carey et al. 2014). A wide spectrum of pyroclastic facies has been reported in submarine successions (e.g. Wright 1996; Wright and Gamble 1999). An emerging problem is related to distinguishing eruption-fed submarine pyroclastic facies from those produced by resedimentation and reworking processes (Cas et al. 1990; Cas and Wright 1991; McPhie et al. 1993; Allen and McPhie 2000, 2009; White 2000; Schneider et al. 2001; Kano 2003; White et al. 2003; Allen and Freundt 2006; Jutzeler 2012; Jutzeler et al. 2014a, b). For eruptions that have not been witnessed, a careful facies analysis of the deposits, together with clast vesicularity and compositional data, offers

Editorial responsibility: V. Manville

Electronic supplementary material The online version of this article (doi:10.1007/s00445-014-0867-x) contains supplementary material, which is available to authorized users.

M. Jutzeler · J. McPhie · S. R. Allen
CODES—ARC Centre of Excellence in Ore Deposits, University of Tasmania, PO Box 79, Hobart 7005, Australia

Present Address:
M. Jutzeler (✉)
National Oceanography Centre, European Way, Waterfront Campus,
Southampton SO14 3ZH, UK
e-mail: jutzeler@gmail.com

a means of reconstructing the eruptive activity and making the eruption-fed versus resedimented distinction. In particular, submarine explosive eruption-fed facies are thought to be characterised by thick to extremely thick, laterally extensive beds composed mainly of angular pyroclasts; the beds may be massive or show weak normal (dense clasts) or reverse (vesicular clasts) grading (McPhie et al. 1993).

The Dogashima Formation on the Izu Peninsula, Japan, was part of the open-marine, rear-Izu-Bonin arc (Tani et al. 2011) during the Pliocene (Fiske 1969; Cashman and Fiske 1991; Tamura et al. 1991; Tamura 1994). Palaeo-temperature measurements on dense clasts in an iconic unit of massive grey andesite breccia in the Dogashima Formation (Tamura et al. 1991), hereafter named D2-2, indicate that these clasts were hot at deposition. This unit grades into white pumice breccia (D2-3), implying synchronous deposition of both units and an eruption-fed origin. Therefore, the facies characteristics exposed at Dogashima provide a guide to infer the critical distinction between explosive eruption-fed and resedimented pumice-rich facies.

High-intensity subaqueous explosive eruptions that produce abundant low-density pumice clasts ('neptunian eruptions'; Allen and McPhie 2009) involve eruption columns that are prone to collapse as a result of the rapid increase in density of single pumice clasts and of the eruption column as the gas (magmatic steam) cools and condenses as a result of mixing with sea water (Kato 1987; Kano 1996; Kano et al. 1996; Allen et al. 2008). The pumice lapilli are then transported away from the vent in cold or lukewarm, water-supported, sea floor-hugging density currents (e.g. Allen et al. 2008; Allen and McPhie 2009). In some cases, temperature and textural data demonstrated that part of the clasts were hot during transport and deposition (Tamura et al. 1991; Kano et al. 1994). In some cases, eruptions may be sufficiently powerful that some of the erupted pyroclasts reach the water surface before being sufficiently waterlogged to sink, creating pumice rafts, such as during the July 2012 Havre eruption (Carey et al. 2014; Jutzeler et al. 2014a, b). Subaqueous pumice-rich eruption columns may produce neutrally buoyant, laterally spreading suspensions of pyroclasts, but these suspensions are composed almost exclusively of pyroclasts with slow settling velocities, such as fine (<2 mm) glass shards, crystals and insufficiently waterlogged, coarse pumice clasts (Kano 2003; Allen and McPhie 2009). Clast rounding may not significantly change during transport in pumice-rich density currents in below wave-base environments, as clast impacts are buffered by water (White 2000), and saturated pumice clasts have specific gravities only slightly above that of water (e.g. Manville et al. 1998, 2002) and are therefore easily mobilised.

The Dogashima Formation exposes outstanding outcrops allowing detailed reconstruction of the eruption sequence from facies analysis. The Dogashima Formation was generated by a combination of pumice-forming explosive eruptions, lava dome growth and destruction and inter-eruptive

sedimentation. In particular, this study examines the relationship between lava clasts issued from the destruction of a hot lava dome and pumice clasts formed by a submarine explosive eruption that destroyed the lava dome.

The Dogashima Formation is also very important because it was deposited in a submarine channel and its overbank, which are well exposed in cross-section. In such island arc settings, the submarine flanks of volcanoes are incised by channels and canyons that focus the downslope movement of sediment and water (e.g. Cas et al. 1990; Gardner 2010; Watt et al. 2012). Complex, channelled sea floor bathymetry and large-scale dune fields are clearly observed around the submerged portions of modern volcanic arcs in swath bathymetry and submarine camera data (e.g. Wright 2001; Gardner 2010). However, access to these modern settings is limited and cross-sections are rarely exposed. Detailed lithofacies information on the volcanoclastic facies that form in and around submarine channels are best obtained from well-exposed and accessible uplifted successions. In the Dogashima Formation, the channel is filled by pumice-rich pyroclastic deposits emplaced by eruption-fed, sea floor-hugging, high-concentration density currents and overlain by cross- and planar-bedded, pumice-rich facies interpreted to result from reworking and resedimentation by high-energy tractional currents in a below wave-base environment.

We present new high-resolution stratigraphic, geochemical, U-Pb ages from zircons, componentry and grain size data for the Dogashima Formation. We use facies characteristics to reconstruct the eruption style and sequence and explore the sedimentation processes operating in the submarine channel in response to the voluminous influx of pyroclasts.

Terminology

The term breccia is non-genetic and used for a clastic aggregate composed mostly of angular clasts >2 mm (Fisher 1961). Matrix is used for components <2 mm. Fine breccia is used hereafter for breccia with an average clast size <10 cm. Fine-grained facies are referred to as pumice sandstone (1/16–2 mm) and shard-rich siltstone (1/256–1/16 mm) without implying genesis. Non- to poorly vesicular (<20 vol% vesicles) clasts are termed dense clasts. Bed thickness terms follow Ingram (1954); the term 'extremely thick' refers to beds >10 m thick. Volume percentages of clasts and grain size distributions of the volcanoclastic facies were calculated by image analysis and functional stereology (Jutzeler et al. 2012). Geochemical and geochronological analyses were carried out at the University of Tasmania (Australia); clast compositions were determined by X-ray fluorescence (XRF) with a Philips PW1480, whereas crystal analyses were performed on a Cameca 100X electron microprobe; the age of the formation was calculated from U-Pb in zircons by laser ablation inductively coupled plasma mass spectrometry (LA-ICP-MS).

Geological setting of the Dogashima Formation

The Dogashima Formation is part of the Miocene-early Pliocene volcanogenic Shirahama Group that covers 500 km² on the Izu Peninsula, Honshu, Japan (Ibaraki 1981; Tamura 1994; Geological Survey of Japan 2010; Tani et al. 2011). The Shirahama Group is part of the northern extension of the Izu-Bonin arc, which is related to the westward subduction of the northwestern margin of the Pacific Plate under the Philippine Plate (Taylor 1992; Tani et al. 2011). Northwestern subduction of the Philippine Plate beneath the Eurasian Plate (including Japan) resulted in collision and uplift of the northern segment of the Izu-Bonin arc (including the Shirahama Group) at ~1 Ma (Huchon and Kitazato 1984).

The Shirahama Group spans 5.5–1.7 Ma (UP b in zircons; Tani et al. 2011) and comprises diverse volcanic and subvolcanic facies (lavas, dykes, cryptodomes and volcanoclastic facies). The succession is a little deformed and virtually unaltered. Most lavas and intrusions range in composition from basaltic andesite to dacite; basalt and rhyolite are rare (Tamura 1994). This group is thought to include the products of at least six scattered and overlapping eruption centres (Sawamura et al. 1970; Kano 1983, 1989; Yamada and Sakaguchi 1987).

Although the environments of eruption and deposition of the Shirahama Group are poorly constrained, the widespread presence of numerous planktonic foraminifera species (e.g. Ibaraki 1981) suggests that an open-marine environment predominated. The abundance of hyaloclastite and pillow lavas throughout the Shirahama Group and in particular in the Matsuzaki Formation (Kano 1983, 1989; Tamura 1990, 1994) also attests to a submarine environment. An undated island may have been present near Shimoda and Shirahama towns, <20 km southeast of the present Dogashima, because conglomerate occurs in the late Miocene Asahi Formation, and the early Pliocene Harada Formation includes cross-bedded, coastal channel facies, calcarenite and limestone (Matsumoto et al. 1985). Gordee et al. (2008) reported undated conglomerate beds that contain charcoal fragments and shells 11 km south of Dogashima, reflecting input from a subaerial island. From rare earth element abundances and mineral assemblages in lavas, Tani et al. (2011) proposed a rear-arc setting for the Shirahama Group, >20 km from the Izu-Bonin volcanic front. This distance from the arc is consistent with the Shirahama Group having accumulated in an open-marine setting. The paucity of subaerially sourced components in formations above and below the Dogashima Formation is also consistent with an open-marine, below wave-base environment that included mostly underwater volcanoes.

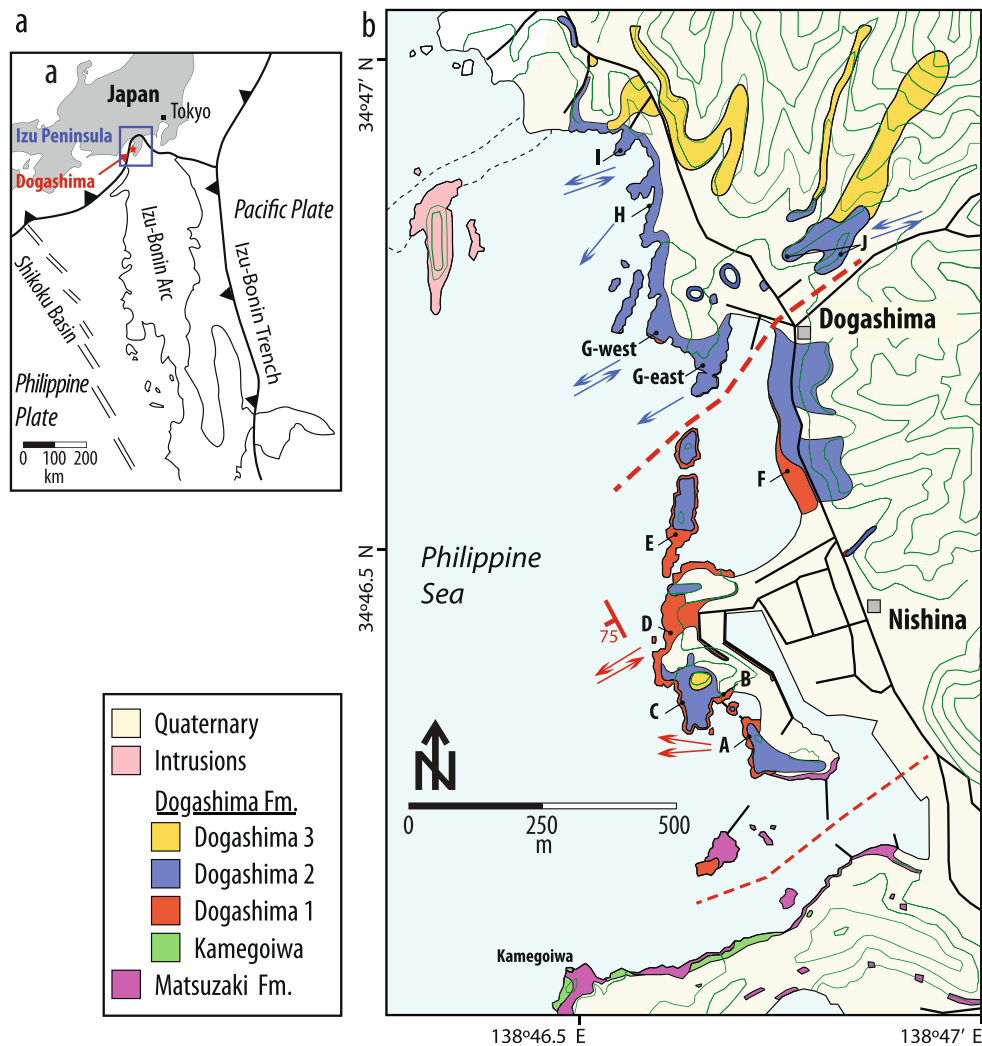
The Dogashima Formation

The Dogashima Formation is exposed over 1.5 km² and is 5 to >80 m thick, suggesting a volume of at least ~10⁷ m³ (Fig. 1). It includes four main subdivisions (Fiske 1969; Tamura 1990, 1994), here named Kamegoiwa, and Dogashima 1, 2 and 3 up stratigraphy (Fig. 2). The formation is dominated by white pumice clasts (overall 80 vol%) and crystal fragments. The succession is a little deformed and virtually unaltered; numerous joints and faults have a constant northerly strike over the whole area and overall show little or no displacement. The stratigraphy of the Dogashima Formation was logged at 12 localities, mostly along the coast. The beds in the Dogashima Formation from localities A–F have a ~5-m vertical offset above the beds of localities G–J, suggesting a sub-vertical fault south of locality G (Fig. 1). Beds in the Dogashima Formation are tilted ~10° northeastwards. The mapped area (Fig. 1) is delimited by sub-vertical faults and intrusions to the north and by the Matsuzaki Formation to the south (Tamura 1994). The Matsuzaki Formation comprises coherent andesite, monomictic andesite breccia and mafic scoria lapilli. Some clasts derived from the Matsuzaki Formation are present in the Dogashima Formation. The Dogashima Formation is intercalated with the Matsuzaki Formation and is distinguished from it by the presence of tabular, pumice-rich units.

Components of the Dogashima Formation

The Dogashima Formation contains numerous, mainly andesitic clast types that differ in colour, vesicularity, mineralogy and composition (Fig. 3; Table 1). Dogashima 1 and Dogashima 2 are dominated by white andesitic pumice lapilli (Fig. 4; Table 1), whereas the underlying Kamegoiwa pumice breccia is dominated by aphyric rhyolitic pumice clasts; Dogashima 3 is dominated by andesite breccia. Many of the coarsest white andesitic pumice clasts (>30 cm) have remnants of quenched margins. Grey andesite clasts are dense; mostly coarse (10–50 cm) and equant, and a few outsized clasts (up to 10 m) occur in groups. Numerous grey andesite clasts are ovoid and have quenched margins and radial joints (Fig. 3a–c); rare (<0.1 vol%) clasts are fluidal (Table 1). In unit D2-2 near the base of Dogashima 2, the thermoremanent temperatures of very coarse, ovoid grey andesite clasts indicate deposition at 450 °C (Tamura et al. 1991). Plagioclase-aphyric andesitic inclusions within the grey andesite clasts are tholeiitic and follow the compositional trend of the Dogashima Formation although they differ petrographically (Fig. 4). Red andesite clasts can be differentiated from the grey andesite clasts only by the colour of their groundmass; both are dense and plagioclase-pyroxene-phyric (15–20 vol% phenocrysts), although the red andesite has slightly higher FeO and lower K₂O compared with the grey andesite (Online Resource 1). The matrix in units of the Dogashima Formation

Fig. 1 Location, geology and stratigraphy in the Dogashima Formation. **a** Simplified map of the Izu Peninsula (Japan) and the Izu-Bonin arc. *Thin line* is the 3,000 mbsl contour. **b** Local geological map of the Dogashima Formation at Dogashima, Japan; *capital letters* are studied localities; *arrows* show palaeo-current directions, their colours correspond to the studied unit; *dip symbol* for syn-sedimentary faults, *thick black lines* for roads; *dashed red lines* for inferred faults. On land contour (in green), spacing is 20 m



is typically composed of crystal fragments (plagioclase, pyroxene) and other particles of identical aspect and composition to the clasts (Table 1); fine (<1/16 mm) components are mostly minor (<5 vol%).

The bulk clast and feldspar compositions of the Dogashima Formation (Fig. 4a, b; Online Resources 1 and 2) match the compositional range of the Shirahama Group (Tamura 1995) and are transitional between its tholeiitic and calc-alkaline series. The white pumice clasts of Dogashima 1 are very similar in mineralogy and composition to those of Dogashima 2, whereas the grey andesite clasts are slightly less evolved than the white pumice clasts (Fig. 4). Rarely, elongate blebs of grey andesite occur within white pumice (Fig. 3e). These similarities strongly suggest that the white pumice, grey andesite and red andesite were co-magmatic. In addition, microprobe analyses of plagioclase phenocrysts in white pumice clasts and grey andesite clasts, plagioclase crystal fragments and plagioclase microlites in the grey andesite clasts from Dogashima 2 are similar and define a single trend (Fig. 4c; Online Resource 2). Overall, the pumice clasts have a higher

loss on ignition (LOI; 6–12.5 wt%; Online Resource 1) compared with dense clasts (LOI \leq 3 wt%) and are also higher in the mobile major elements K_2O and Na_2O . Zircons in the white pumice clasts and grey andesite clasts in Dogashima 1 and 2 give an age of 4.55 ± 0.87 Ma (U-Pb analysed by LA-ICP-MS; Online Resource 3), consistent with the age of other nearby formations in the Shirahama Group (Tani et al. 2011).

Hydrothermally altered volcanic clasts are a minor but ubiquitous component in the Dogashima Formation and are up to >2 m in diameter. Many units in Dogashima 1 and 2 include clasts identical to those present in the underlying successions, such as white aphyric pumice from the Kamegoiwa pumice breccia and dark andesite clasts from the Matsuzaki Formation. The dark andesite clasts of the Matsuzaki Formation and the coarsely porphyritic andesite clasts in Dogashima 3 are similar in composition to the grey andesite clasts of Dogashima 2 (Fig. 4). White aphyric pumice clasts are angular tube pumice up to 40 cm in diameter. The grey scoria clasts and white aphyric pumice clasts are distinct from the compositional field of the other clasts of the

Fig. 2 Coastal outcrops of the Dogashima Formation. **a** Onlap and interfingering contact between the Dogashima Formation and the Matsuzaki Formation (*M*) at locality A. The formations have a regional $\sim 10^\circ$ tilt eastwards (to the *right*), but here shows gentle primary dip to the west. Dark andesite clasts (*blue arrows*) of the Matsuzaki Formation are present in the polymictic volcanic breccia beds (D1-3 and D1-8) of Dogashima 1. Massive grey andesite breccia (D2-2) has an irregular contact with the basal polymictic volcanic breccia (D2-1); photo courtesy S.M. Gordee. **b** Major tabular units in Dogashima 1 (D1) and Dogashima 2 (D2) at locality D (Fig. 1); pumice breccia (D1-2, D1-5), cross-bedded pumice breccia (D1-1, D1-12), dark grey polymictic volcanic breccia (D1-3) and massive grey andesite breccia (D2-2). Coarse white pumice clasts (*white arrows*) at the base of the polymictic volcanic breccia (D1-3) in Dogashima 1 were eroded from underlying bed D1-2. **c** Dogashima Formation at locality C (Fig. 1). Note sharp contacts at the base and top Dogashima 2 (D2). *Black arrows* show coarse grey andesite clasts in massive grey andesite breccia (D2-2), *white arrow* points to lens of coarse white pumice clasts in pumice breccia (D2-3). Note the gradational contact between the massive grey andesite breccia (D2-2) and the pumice breccia (D2-3) in Dogashima 2. *Blue arrow* points to coarse white pumice clasts in polymictic volcanic breccia of Dogashima 1. *D3* Dogashima 3

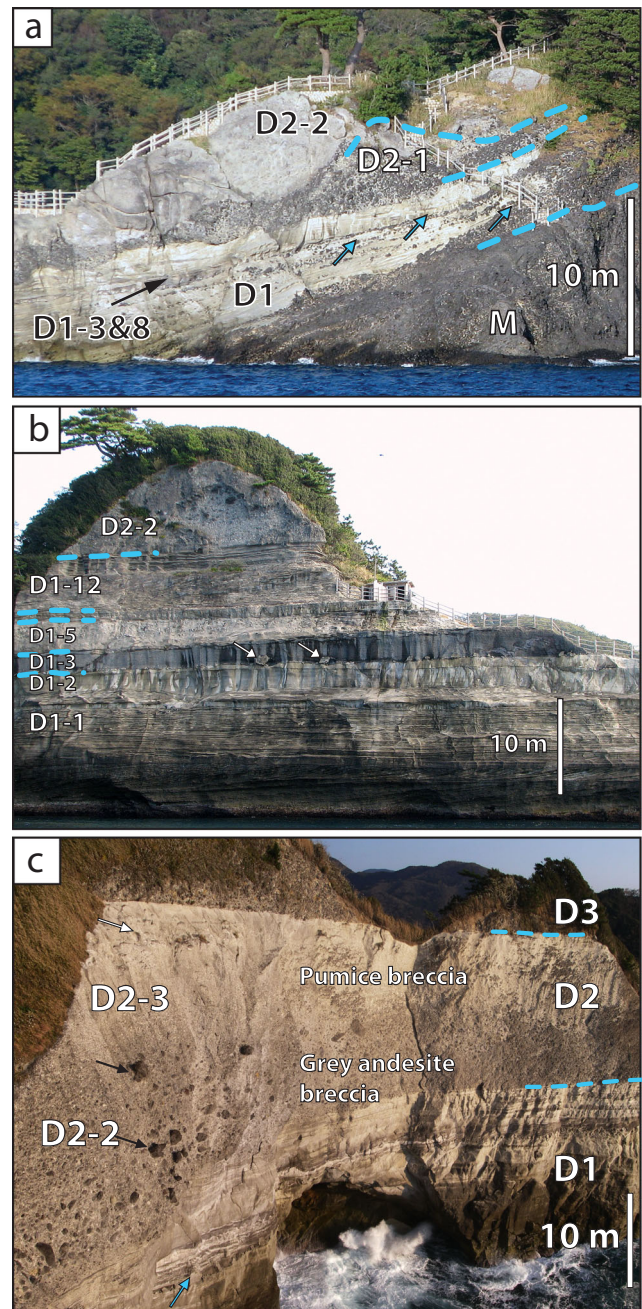
Dogashima Formation, although they fall within the overall trend of the Shirahama Group (Fig. 4). The coarsely porphyritic andesite clasts in Dogashima 3 contain more phenocrysts and have a coarser groundmass than the grey andesite clasts in Dogashima 2. No palaeo-temperature data are available for the coarsely porphyritic andesite clasts.

Kamegoiwa pumice breccia

The Kamegoiwa pumice breccia is up to 10 m thick and exposed over few outcrops in the southern part of the studied area (locality K, Figs. 1, 5 and 6). It is intercalated within the Matsuzaki Formation, overlying brown scoria beds and underlying lavas. The Kamegoiwa pumice breccia consists of two internally stratified pumice breccia beds composed of white aphyric pumice clasts. At the base, there is a high concentration of brown scoria clasts derived from the Matsuzaki Formation (Fig. 7). The matrix is chiefly composed of crystal fragments; grey-banded pumice and hydrothermally altered volcanic clasts are common. Although bed contacts are hidden by sea level, lavas/intrusions of the Matsuzaki Formation and faults, the presence of white aphyric pumice clasts from the Kamegoiwa pumice breccia in Dogashima 1 and 2 indicates that it was un lithified and exposed on the sea floor at the time of deposition of Dogashima 1 and 2.

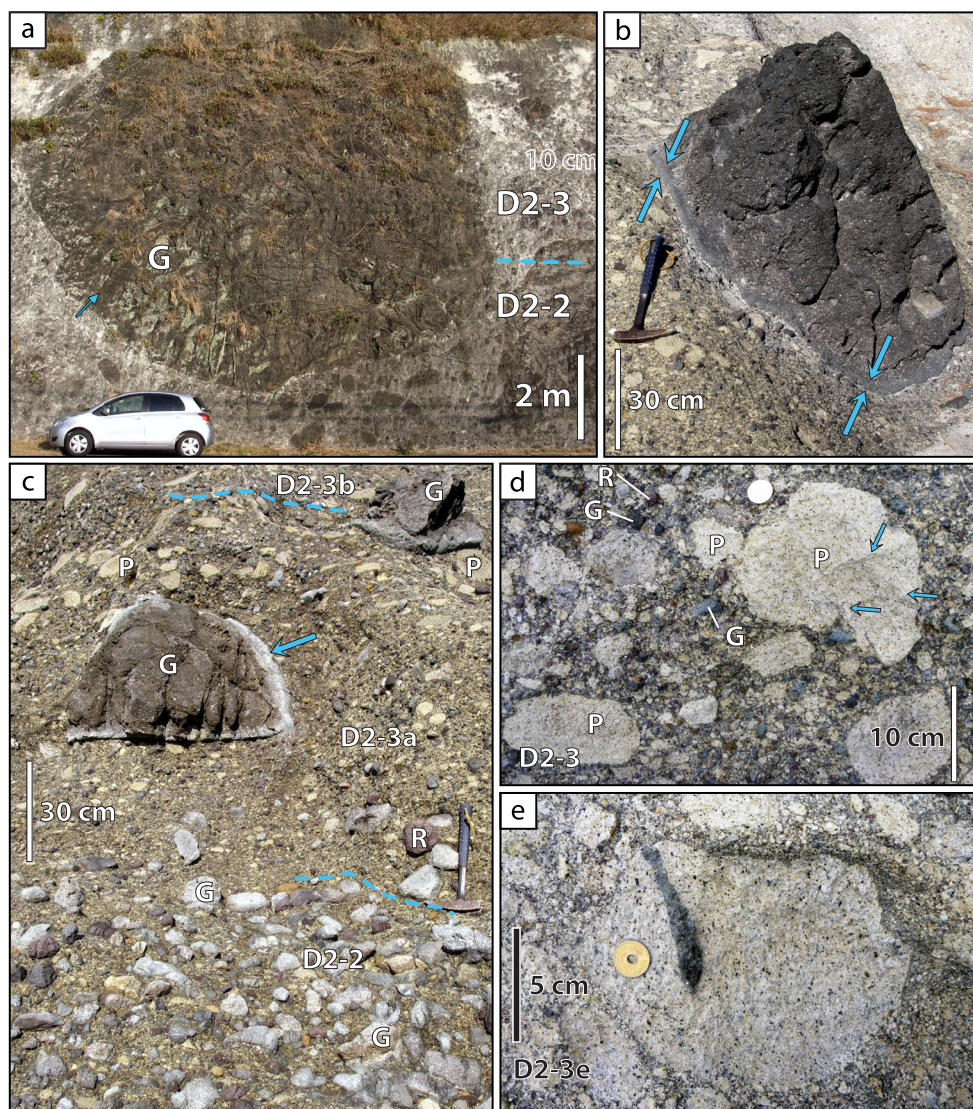
Dogashima 1

The pumice-rich Dogashima 1 is >15 m thick, mostly exposed in the southern part of the studied area, and overlies the Matsuzaki Formation at locality A with an erosional contact



(Figs. 1, 2, 5 and 6; Table 2). Dogashima 1 is composed of multiple, laterally extensive or lenticular, thick graded beds of pumice breccia (Fig. 8a, b); thin to very thick cross-bedded, planar-bedded and normally graded pumice breccia/sandstone (Fig. 8c, d); medium to very thick beds of polymictic volcanic breccia (Fig. 8b, e, f); and thin to medium beds of shard-rich siltstone (Table 2). From localities A to E, the bases of two polymictic volcanic breccia beds in Dogashima 1 are sharp, discordant surfaces that truncate the underlying beds, indicating erosion, in particular at localities A and B (Figs. 2a, b and 8b, e).

Fig. 3 Examples of clasts of Dogashima 2. **a** Outsize grey andesite clast (*G*), in the massive grey andesite breccia (D2-2), overlain by pumice breccia (D2-3), locality F. Note the weak columnar joints (*blue arrow*). **b** Outsize grey andesite clast in the pumice breccia (D2-3) with well-developed quenched rim (*blue arrows*). **c** Sharp transition from the massive grey andesite breccia (D2-2) to basal beds of the pumice breccia (D2-3). The coarse grey andesite clast has a quenched rim (*blue arrow*), locality G-east. *P* white pumice, *G* grey andesite, *R* red andesite. **d** Coarse white pumice clasts (*P*) with rough radial joints (*blue arrows*) and much smaller grey andesite (*G*) and red andesite (*R*) clasts in pumice breccia (D2-3). **e** Rare clast of white pumice containing an elongate blob of grey andesite; contact of the two magmas is sharp. D2-3e locality G-east



Dogashima 2

Dogashima 2 is 15 to 30 m thick, covers the whole area and is composed of eight stratigraphic units (Figs. 5 and 6; Table 2). It is dominated by white pumice clasts (chiefly 60–95 vol%). The most prominent units are the grey andesite breccia (D2-2) and the overlying pumice breccia (D2-3) that are separated by a gradational to sharp contact (Figs. 2c, 3a and 9a). The basal contact of Dogashima 2 is a 600-m-wide, 15-m-deep disconformity carved into beds of Dogashima 1. At locality A (Fig. 2a), Dogashima 2 directly overlies a disconformable contact on coherent andesite and monomictic andesite breccia of the Matsuzaki Formation. Palaeo-lows (>50 m wide) are visible at localities G-east and G-west (Fig. 9) and between localities A and B. The disconformity is less pronounced in the northern localities H and I where Dogashima 2 overlies the stratified pumiceous facies of Dogashima 1.

The main basal unit (D2-2) is very thick (up to 7 m) massive grey andesite breccia (D2-2) that occurs over the southern and central part of the study area between localities A to G-east (Figs. 3a, 5 and 9a; Table 1). Unit D2-2 has a sharp, discordant contact with Dogashima 1 and is dominated (up to 90 vol%) by coarse, grey andesite clasts, some of them with quenched margins and rare fluidal shapes. Very coarse (1–10 m) grey andesite clasts occur in clusters that show overall coarse-tail reverse grading. At locality A, D2-2 overlies polymictic volcanic breccia (D2-1) that contains dark andesite clasts of the Matsuzaki Formation (Fig. 2a). Here, D2-2 also contains conspicuous hydrothermally altered volcanic clasts as well as grey andesite clasts and is finer grained (average 16 cm) than at the other localities (average 25–50 cm). The presence of chilled margins on grey andesitic clasts in massive grey andesite breccia in the middle of the formation (unit D2-2 in this paper; Fig. 3) and thermoremanent temperatures of 450 °C in clast rims (at 5 cm depth in the

Table 1 Characteristics of clasts in the Dogashima Formation

Table clasts in the Dogashima Formation				
Clast	Occurrence	Colour, shape	Size; vesicularity	Phenocryst assemblage
White pumice	Abundant in D1 and D2, rare in base of D3	White, slight yellowish hue. Mostly angular and curvilinear, rounded in D2-2 and sub-angular to sub-rounded in D2-6 and D2-8. Common quenched rim and rare bread-crust texture in coarse (>50 cm) clasts	Mostly <8 cm; max. 1.50 m. Elongate vesicles (>60 vol%) partially preserved.	<40 vol% phenocrysts. Plagioclase is dominant (25–35 vol%, average ~1 mm, max. 3 mm; An48–70). Clinopyroxene, orthopyroxene and opaque phases are subordinate (<5 vol%) and are no more than 0.5 mm in size; quartz phenocrysts are very rare (<0.1 vol%). Phenocrysts are equant and typically broken on one face and are also found as clusters. Glass is chiefly devitrified
Grey andesite	Dominant in D2, minor in lower D3	Grey to dark grey, unaltered and chiefly equant. Coarse clasts (>50 cm) are equant to ovoid, have quenched rims several centimeters wide and internal radial joints. Rare (<1 vol%) fluidal clasts are present	Mostly 10–50 cm (but up to 10 m) in D2-2; <10 cm in D2-3. Non-vesicular	15–20 vol% phenocrysts, which is similar to dense rock equivalent of white pumice clasts. Plagioclase crystals (10–15 vol%; An49–57) are equant, euhedral and 1–2 mm long, although rare clusters are up to 10 mm across. Clinopyroxene (2 mm), orthopyroxene (1 mm) and oxides (1 mm) are subordinate (<5 vol%) and form aggregates. Trachytic groundmass texture defined by 0.5–1 mm feldspar microlites (An53–69). Scattered, ovoid weakly porphyritic inclusions up to a few centimeters across occur
Crystal fragments	D1 and D2	Commonly equant in shape, broken on one to many faces	Mostly 1/16–2 mm	Mostly plagioclase (An51–70); minor clinopyroxene and orthopyroxene
Red andesite	D2-1, D2-2 and D2-3	Red, angular to sub-rounded, equant in shape	Mostly <10 cm. Maximum size 30 cm	Phenocryst content and plagioclase composition (An64–78) match those of grey andesite clasts
Hydrothermally altered volcanic clasts	D1, D2, minor in base of D3	Ochre-yellow, brown, dark red or red; angular to sub-rounded andesite, scoria and rare sub-rounded clasts of pumice breccia	Mostly <10 cm. Outsized (>3 m) altered pumice breccia in D2-2 Dense to formerly vesicular	Variable mineralogy; mostly composed of plagioclase
Dark andesite	Minor in beds of D1 at locality A and bed D1-3/8 at locality B. Dominant in Matsuzaki Fm	Black, with brown, glassy groundmass; very angular	Mostly 10–20 cm Poorly vesicular (<10 vol%)	Dominantly plagioclase and opaque phases (0.5–1.5 mm; 20 vol%). Lath-shaped plagioclase micro-phenocrysts (0.1–0.2 mm; >50 vol%) also occur
White aphyric pumice	Rare to minor in some D1 and D2 beds. Dominant in Kamegoitwa and some other beds	White, commonly rounded but angular in some beds	Mostly <6 cm Tube vesicles (~60–80 vol%) overall finer and more elongate than in the white pumice	Almost aphyric; rare plagioclase (<1 vol%) is 0.1 mm (1 mm max). The glass is chiefly devitrified
Grey scoria	Minor in D1-3 and D1-8. Minor in some beds of Matsuzaki Fm	Pale grey; broken angular pieces of fluidal clasts	Mostly <6 cm. Maximum ~10 cm Moderately vesicular (<50 vol%); vesicles mostly ellipsoidal, weakly aligned (<0.2 mm, max. 3 mm)	Minor phenocrysts (<10 vol%) including plagioclase (max. 2 mm), clinopyroxene and orthopyroxene and rare hornblende
Coarsely porphyritic andesite	Dominant in D3	Grey; angular	Almost exclusively 20–50 cm	

Table 1 (continued)

Table clasts in the Dogashima Formation

Clast	Occurrence	Colour, shape	Size; vesicularity	Phenocryst assemblage
Grey-banded pumice	Common in Kamegoiwa	Grey, flow-banded with dark and pale domains; angular	Very poorly vesicular (<0.5 vol%)	Phenocrysts (>25 vol%) are mostly plagioclase (1 mm and few crystals up to 10 mm), with minor clinopyroxene and orthopyroxene and opaques. Groundmass is fine-grained (<0.1 mm) and composed of feldspar and subordinate clinopyroxene and orthopyroxene and opaques
			3–12 cm long, porphyritic	Phenocrysts (>25 vol%, up to 3 mm) are mostly feldspar and ferromagnesian

clast) at deposition led Tamura et al. (1991) to interpret this unit as the deposit of a ‘hot pyroclastic debris flow’.

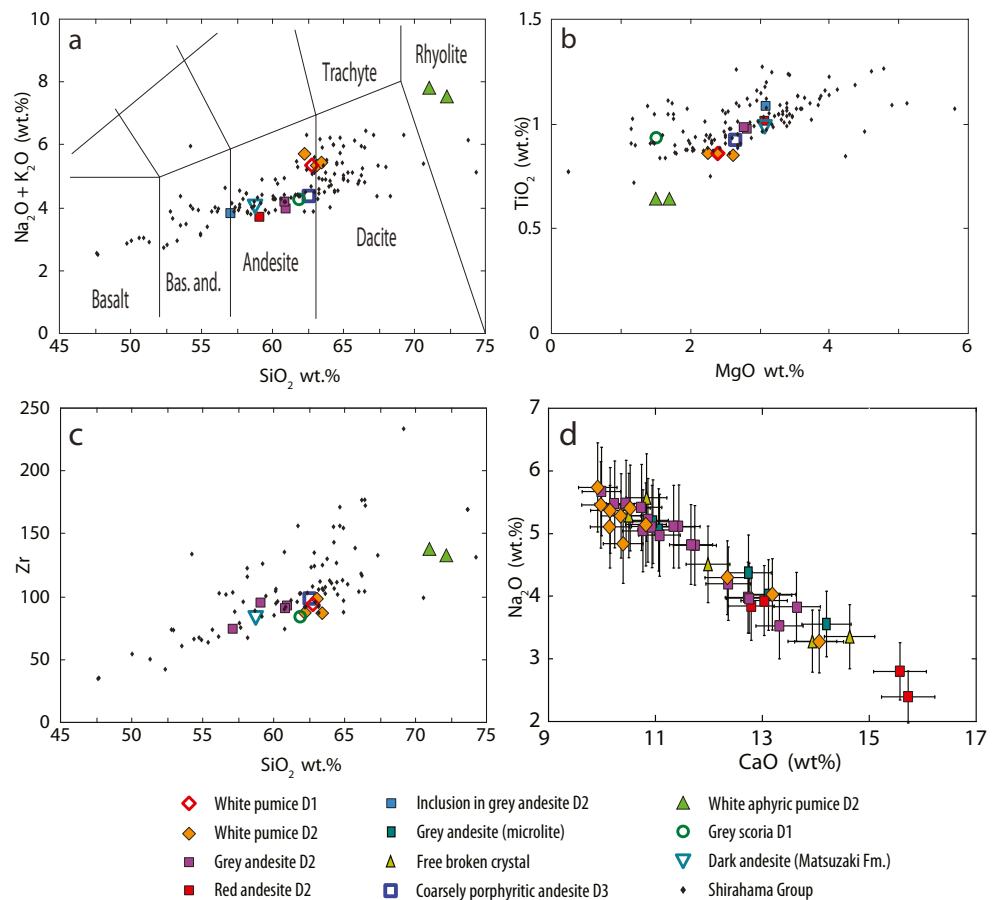
D2-2 is overlain by a 6- to 10-m-thick pumice breccia unit (D2-3) with a sharp to gradational lower contact, depending on the locality (Table 2; Figs. 2c, 3c, 5 and 9a). The pumice breccia is exposed over the central and northern parts of the study area, between localities C and I; its original distribution to the south (localities A, B) is unknown as D2-2 is the uppermost preserved layer (Fig. 2a). D2-3 mostly consists of white pumice clasts (>20–30 vol%) in a matrix of finer (<2 mm) pumice and plagioclase and pyroxene crystal fragments; sub-ordinate grey andesite clasts and minor hydrothermally altered volcanic clasts occur throughout (Tables 1 and 2). D2-3 exhibits very strong lateral facies variations. It is massive to normally graded in its southernmost exposures (localities C to F), stratified and reversely graded at locality G-east and internally stratified and finer grained in the northern part of the studied area (localities G-west, H and I; Figs. 6 and 9b, c). The upper part of the pumice breccia (beds D2-3d and D2-3-e) at locality G-east is reversely graded and shows strong bimodality in the size of pumice (coarse) and dense (fine) clasts, reflecting a hydraulically well-sorted deposit (Fig. 10c, d). In general, D2-3 overlies D2-2; however, at locality G-east, a 1-m-thick, ~5-m-long lens of pumice breccia with similar texture and composition to D2-3 occurs below D2-2 (Fig. 11). At G-east, D2-3 is overlain with a gradational contact by medium to thick beds of planar-stratified pumice breccia (D2-4; Fig. 9a, c) and by a very thick, diffusely stratified, fine pumice breccia (D2-5; Fig. 9a, b) in sharp contact with D2-4.

Localities G-west to I provide the most complete exposure of the upper part of Dogashima 2, which comprises tabular to lenticular, cross-bedded pumice breccia-conglomerate (D2-6), planar-bedded pumice breccia (D2-7) and cross-bedded pumice breccia-conglomerate (D2-8) at the top (Table 2; Figs. 5, 6, 9b and 12). At localities H and I, exceptional bimodality in the size of pumice clasts characterises the planar-bedded pumice breccia (D2-7); very coarse pumice clasts (up to 1 m) occur in a diffusely stratified matrix chiefly composed of white pumice clasts (mostly <2 mm). At localities C, I and J, Dogashima 2 is separated from the weakly stratified andesite breccia of Dogashima 3 by a sharp erosional contact (Figs. 2c and 5).

Dogashima 3

Dogashima 3 is made of a >50-m-thick, weakly stratified andesite breccia. The breccia comprises coarsely porphyritic andesite clasts in a white pumice sandstone matrix (Table 2). It is mostly preserved in the northern part of the area; a 5-m-thick remnant occurs at the top of locality C (Fig. 2c). Its upper boundary has not been identified due to vegetation cover and/or erosion.

Fig. 4 Clast analyses in the Dogashima Formation and Shirahama Group (Online Resources 1 and 2). **a** Total alkalis versus silica (TAS) diagram for clasts in the Dogashima Formation; compositional fields after Le Bas et al. (1986); Shirahama Group data from Tamura (1990, 1994, 1995). **b**, **c** TiO_2 versus MgO and Zr versus SiO_2 diagrams for clasts in the Dogashima Formation, compared with Shirahama Group analyses, respectively. Plotted compositions are recalculated to 100 wt% anhydrous. D1, D2 and D3 for Dogashima 1, Dogashima 2, and Dogashima 3, respectively. **d** Microprobe analyses of rims and cores of plagioclase crystals in Dogashima 2. Compositions of plagioclase phenocrysts from various origins define a single trend, consistent with a comagmatic source



Grain size and components of Dogashima 2 at locality G-east

The coarse (modes mostly >2 mm) grain size fraction of 10 nested (assemblage of images at different magnifications) samples from D2-2 to D2-6 at locality G-east has been documented with image analysis and functional stereology (Jutzeler et al. 2012) to quantify the grain size distribution in volume and weight percent (Fig. 13). Three samples (base, middle, top) were analysed from bed D2-3e where Cashman and Fiske (1991) identified good hydraulic sorting.

Samples from the massive grey andesite breccia at the base (D2-2) to the middle of the D2-3 pumice breccia (D2-3e base) show normal size grading in dense components (Fig. 13a), whereas beds D2-3c–d and D2-3e are reversely graded in pumice clast size. Dense clasts decrease continuously in abundance from the basal unit D2-2 (50 vol%) upwards to unit D2-5 (<10 vol%; Fig. 13c) and are more abundant (20 vol%) in D2-6. Pumice clasts are almost absent (<5 vol%) in unit D2-2 but make up to 20–30 vol% of the overlying pumice breccia units. The matrix and cement (<2 mm) proportion ranges between 50 and 80 vol%. Coarse (>16 mm) clasts are abundant only in the lower part of the succession (D2-2; 40 vol%), and their volume decreases to <5 vol% in D2-2; they form a small percentage of the clasts (<2 vol%) in D2-6. Most units

have a unimodal grain size distribution between -2 and -3 phi (4–8 mm), although D2-2 is coarser (-5 phi; 32 mm) and in unit D2-3c, pumice clasts show a bimodal grain size distribution (-4 and -2.25 phi; 16 and 5 mm). In the middle of bed D2-3e, the grain size distribution in weight percent shows that pumice clasts are consistently coarser than dense clasts (Fig. 13a).

A submarine channel in the Dogashima Formation

Between the southern localities A and G-east, the basal disconformity and internal architecture of Dogashima 2 indicate deposition in a palaeo-sea floor channel more than 600 m wide and up to 15 m deep eroded into beds of Dogashima 1 and filled by units of Dogashima 2 (Fig. 11). Within the channel, the massive grey andesite breccia (unit D2-2) is especially thick and has a fully gradational to sharp contact with the overlying pumice breccia (unit D2-3, localities B, C and F). Further north (localities G-east to I), the overbank setting is characterised by much thinner (<1 m), finer grained and commonly stratified pumice breccia (D2-3) and cross-bedded pumice breccia-conglomerate (D2-6). In particular, the coarse grey andesite clasts and the massive grey andesite

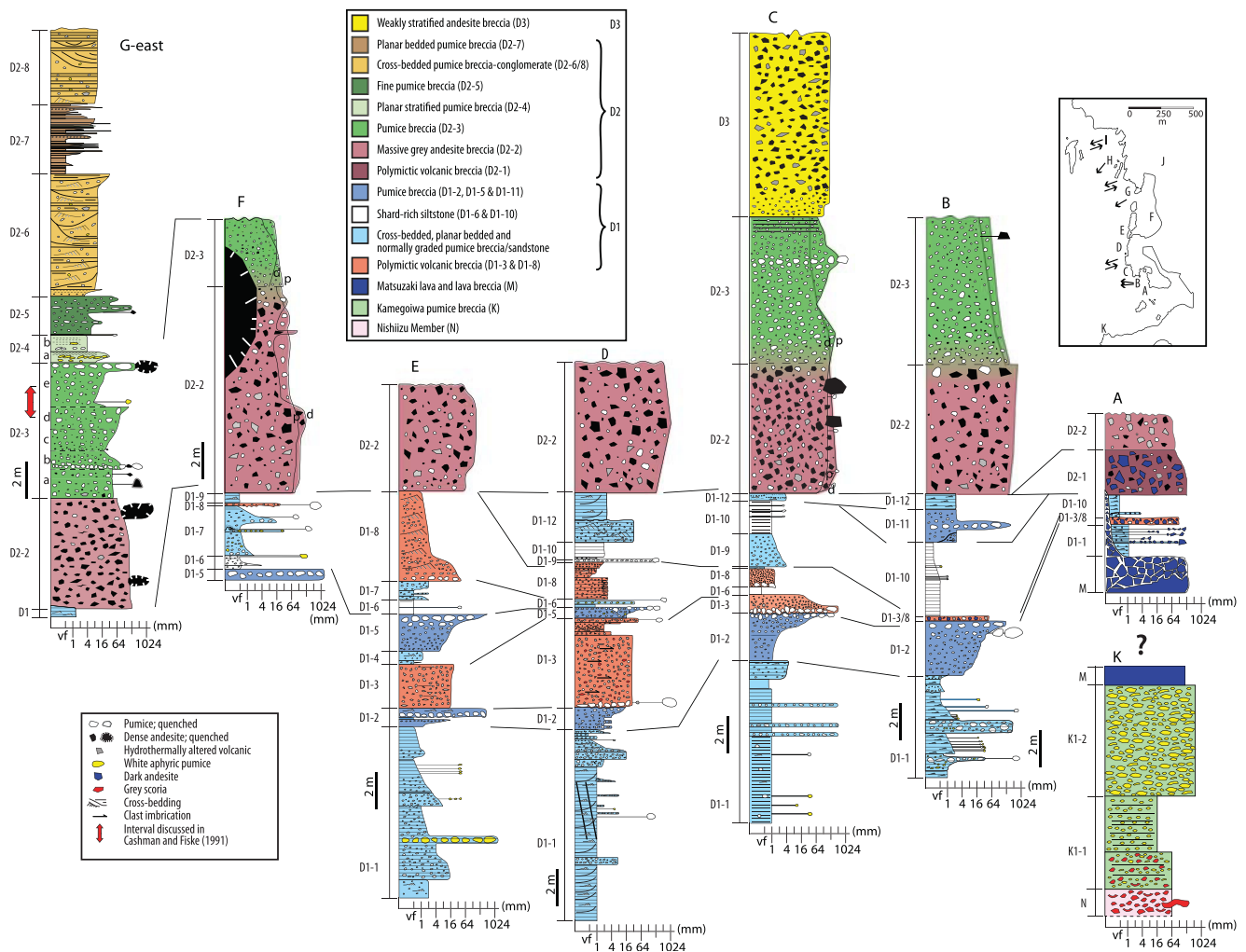


Fig. 5 Stratigraphic logs of the southern part of the Dogashima Formation (localities A to G-east), displayed north (left) to south (right). Inset shows localities and palaeo-flow directions on a simplified map (Fig. 1). All log bases start at sea level; *d* dense clast, *p* white pumice clast

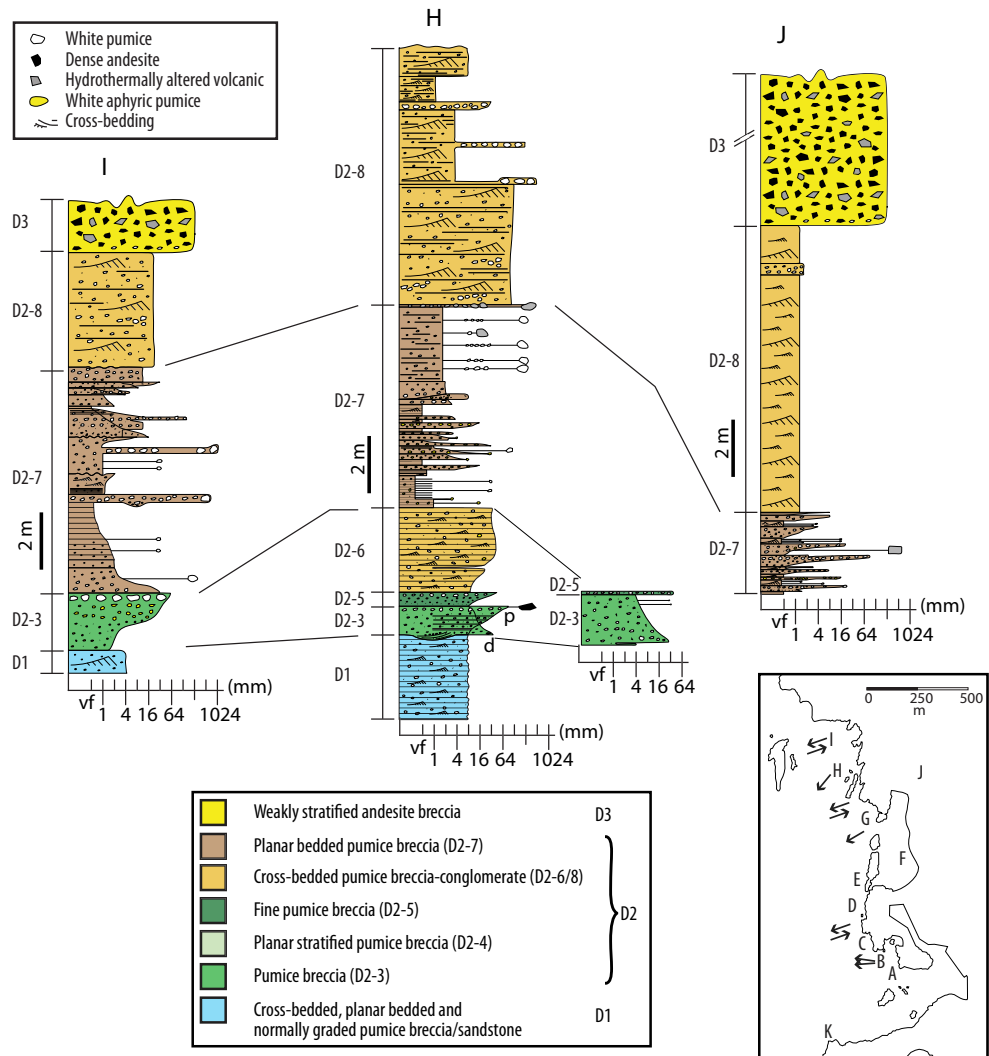
breccia (unit D2-2) are absent. At locality A, Dogashima 1 pinches out, reducing from ~10 to <3 m thick, and the massive grey andesite breccia (D2-2) is thinner (at the expense of D2-1) where it onlaps the constructional morphology of the Matsuzaki Formation andesite (Fig. 2a).

The submarine channel floor between localities A and G-east includes two palaeo-bathymetric lows. The main palaeo-low occurs at localities E, F and G-east, and a less pronounced, ~5-m-deep palaeo-low occurs between localities A and B (Fig. 14). A palaeo-high is present between the two palaeo-lows, over localities C, D and E, where Dogashima 1 is 15–25 m thicker than at localities A, F and G-east (Fig. 5). However, the difference in thickness is exaggerated on the sub-vertical cliffs by a general tilt of the whole Dogashima Formation by ~10° towards the east.

Elongate pumice clasts that show parallel orientation and/or imbrication of clast long axes (Table 3) were used as palaeo-current indicators. Throughout the Dogashima area

(Fig. 1), these palaeo-current indicators imply an overall northeast to southwest palaeo-current direction and, at locality B, an east to west current direction. The channel axis (though not known in detail) appears to have been roughly parallel to this palaeo-current trend, so it is reasonable to infer that the currents producing the palaeo-currents indicators were focussed in the channel (Fig. 14). Syn-depositional normal faults in Dogashima 1 at locality D (Fig. 12f) indicate a palaeo-slope towards the southwest, which is consistent with southwesterly directed palaeo-currents. However, many cross beds imply opposite palaeo-current directions (northeast to southwest and southwest to northeast), including some small-scale (<50 cm thick) compound (i.e. internally cross-stratified; McKee and Weir 1953; Allen 1963) cross beds in unit D2-8 (Fig. 12e). Opposite palaeo-current directions are interpreted to be associated with current reflections and/or up and down currents within the channel, backsets and/or antidunes. Pumice clasts in cross-bedded and planar-bedded facies do not show extensive rounding textures characteristic of

Fig. 6 Stratigraphic logs of the northern part of the Dogashima Formation (localities G-east to I), displayed north (left) to south (right). Inset shows localities and palaeo-flow directions on a simplified map (Fig. 1). Bases of logs H and I start at sea level; *d* dense clast, *p* white pumice clast; see Fig. 5 for symbol key



abrasion in above wave-base setting (e.g. White et al. 2001; Manville et al. 2002). We interpret that Dogashima 2, and in fact all of the Dogashima Formation, was deposited in a below wave-base region where strong ocean currents occurred,

consistent with a submarine channel setting. This interpretation matches the open-marine setting and absence of above wave-base facies (e.g. conglomerate) in proximity to the Dogashima Formation.

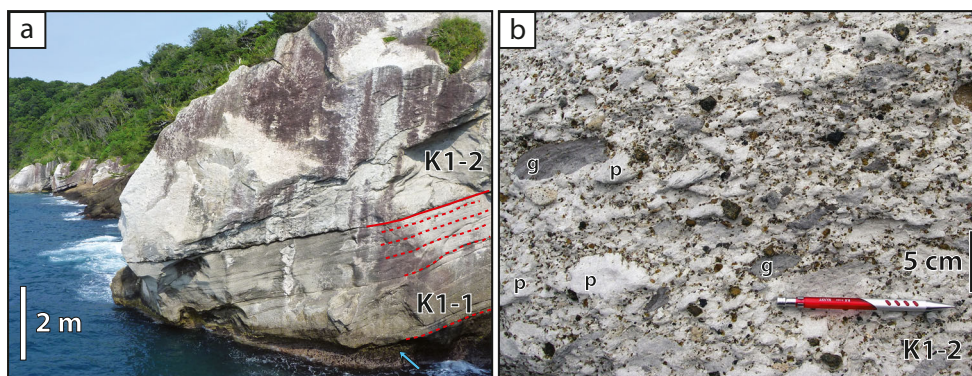


Fig. 7 Kamegoiwa pumice breccia, locality K. **a** Base of Kamegoiwa pumice breccia (K1-1) is strongly stratified and includes high abundance of clasts from the underlying Matsuzaki Formation (blue arrow). K2-2 is coarser grained, weakly stratified and locally reversely graded. **b** White

aphyric pumice (*p*) and crystal fragments are the dominant clast types in the upper unit of the Kamegoiwa pumice breccia (K2-2). Grey banded pumice clasts (*g*) and hydrothermally altered volcanic clasts are common. Note the near-absence of matrix

Table 2 Characteristics of facies in the Dogashima Formation

Beds, occurrence	Bed characteristics	Clast characteristics	Origin
Kamegoiwa			
Pumice breccia K1-1, K1-2 <i>Locality: K</i>	Very thick (up to 10 m) sequence made of 2 stratified units separated by sharp contact boundary. K1-1 occurs locally, whereas K1-2 is present at all outcrops. The pumice breccia is in erosional contact with underlying units of the Matsuzaki Formation and lowermost beds (up to 2 m thick) contain high concentration of scoria clast picked up from the Matsuzaki Formation. The lowermost unit K1-1 (5 m) is fine stratified breccia; K1-2 (5 m) is reversely graded, stratified pumice breccia	Angular white aphyric pumice (>70 vol%), sub-dominant crystal fragments, hydrothermally altered volcanic clasts (10 vol%) and flow-banded pumice clasts (<5 vol%). Up to 50 vol% of grey scoria at contact with the Matsuzaki Formation Average grain size 1–2 cm (K1-1) and 1–16 cm (K2-2); maximum 40 cm	Explosive eruption-fed
Dogashima 1			
Pumice breccia D1-2, D1-5, D1-11 <i>Localities: B, C, D, E</i>	Thick to very thick; reversely or normally graded. Tabular, massive and in sharp contact with other units; the top contact is discordant at many localities. Contains lenses of coarse white pumice clasts	Mostly angular white pumice (>60 vol%), sub-dominant crystal fragment, minor angular hydrothermally altered volcanic clasts, rare white aphyric pumice (<1 vol% clasts). Commonly consists of 20–40 vol% of sand-sized clasts Average grain size 0.05–20 cm; maximum 120 cm	Explosive eruption-fed
Shard-rich siltstone D1-6, D1-10 <i>Localities: A, B, C, D, E, F</i>	Thin to medium. Massive to laminated; load, liquefaction-convolution (Table 1) and ball-and-pillow structures occur. Overlies other beds at sharp boundaries. The top contact is commonly an erosion surface	Mostly devitrified glass shards; minor coarse white pumice clasts and free broken plagioclase crystals Average grain size: <0.0063 cm	Explosive eruption-fed
Polymictic volcanic breccia D1-3, D1-8 <i>Localities: A, B, C, D, E, F</i>	Medium to very thick (max. 5 m); stratified, normally or reversely graded, or cross bedded. Well-sorted. Tabular and laterally continuous and merge into a single <50-cm-thick coarse bed at 100 m southeastward of locality C. Basal contact is sharp, discordant and erosional; pinches out above Matsuzaki Formation at locality A. Coarse white pumice clasts can occur in D1-3, probably derived from top of D1-2	Very angular to angular hydrothermally altered volcanic clasts, grey scoria, white aphyric pumice, white pumice, dark andesite. D1-8 rich in rounded white pumice clasts (max. 40 cm) Average grain size 0.5–4 cm; max. 120 cm	Resedimented
Cross-bedded, planar-bedded and normally graded pumice breccia/sandstone D1-1, D1-4, D1-7, D1-9 and D1-12 <i>Localities: A, B, C, D, E, F</i>	Thin to very thick (max. >2 m); cross-bedded in trough or planar-bedded, commonly laminated, or normally graded. Occur in stacks of low angle, lenticular sets of trough cross beds with metres to 10 m wavelengths and amplitudes up to 2 m. Numerous sub-vertical syn-sedimentary normal faults occur in a ~2-m-thick cross-bedded pumice sandstone bed in unit D1-1 at locality D. The faults dip towards the SE and have a vertical displacement of <20 cm	Mostly angular to sub-rounded white pumice; minor hydrothermally altered volcanic clasts, crystal fragments, white aphyric pumice. Outsized white pumice and white aphyric pumice clasts (both up to 1.5 m) spread throughout the beds, or concentrated in single-clast-thick beds. Scattered dark andesite clasts occur in beds in contact with the Matsuzaki Formation at locality A Average grain size: <0.2–6 cm; max. 150 cm	Resedimented
Dogashima 2			
Basal polymictic volcanic breccia D2-1 <i>Locality: A</i>	Thick to very thick (<3 m); massive, in lense (<10 m long). Basal erosive contact that scours (1 m deep, 2 m wide) D1. Contact with overlying D2-2 is sharp and irregular	Mostly angular dark andesite (0–60 vol%) and grey andesite (20–30 vol%); minor hydrothermally altered volcanic clasts, red andesite and rounded white pumice (<3 vol%) crystal fragments. Dark andesite absent from lowermost 30 cm of the unit Average grain size 5–50 cm; max. 80 cm	Explosive eruption-fed
Massive grey andesite breccia D2-2	Very thick (up to 7 m); massive to reversely graded. The basal contact is sharp and discordant	Mostly angular grey andesite (>90 vol%); minor hydrothermally altered volcanic clasts, rounded	Explosive eruption-fed

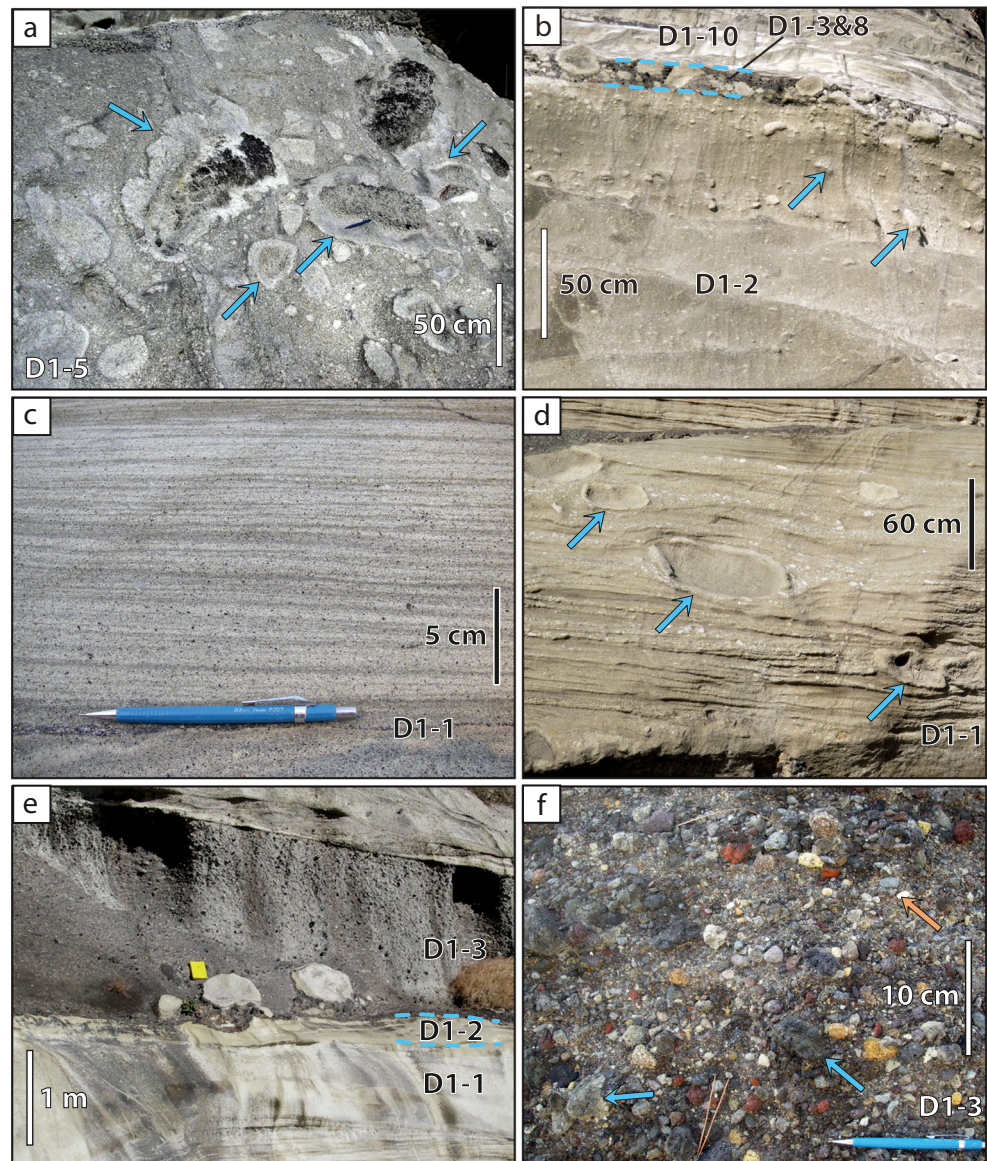
Table 2 (continued)

Beds, occurrence	Bed characteristics	Clast characteristics	Origin
<i>Localities: A, B, C, D, E, F</i>	with D1 and with D2-1 at locality A; it overlaps the Matsuzaki Formation at locality A. Minimum volume estimated at 1×10^6 m ³	white pumice (up to 5 vol%), red andesite; fluidal grey andesite (0.1 vol%) at locality F. Outsized grey andesite clasts (up to ~10 m in diameter) mainly occur in groups in the upper part of the unit at all localities. Locality F: thermoremanence of some of the coarse grey andesite clasts show deposition at >450 °C (Iamura et al. 1991)	
Massive grey andesite breccia D2-2 <i>Locality: G-east</i>	Very thick; massive to normally graded, with groups of quenched outsized andesite clasts. Basal contact is sharp and erosive with D1. Pinches out sharply at this locality	Average grain size 5–50 cm Mostly angular grey andesite; minor hydrothermally altered volcanic clasts (<5 vol%), rounded white pumice (up to 5 vol%), red andesite, fluidal grey andesite (<1 vol%) Outsized grey andesite clasts (up to ~5 m in diameter) mainly occur in groups in the upper part of the unit at all localities	
Pumice breccia D2-3 <i>Localities: B, C, F</i>	Very thick (6–10 m); overall massive to normally graded, with diffuse, coarse lenses of white pumice clasts. Top of unit commonly stratified. Conformable with D2-2, fully gradational. Gradational contact with D2-2 shown by high concentrations of grey andesite and hydrothermally altered volcanic clasts identical to those found in D2-2. Minimum volume estimated at 2.5×10^6 m ³	Average grain size 5–50 cm; max. 400 cm Mostly angular white pumice, grey andesite, crystal fragment. Minor hydrothermally altered volcanic clasts and white aplyric pumice	Explosive eruption-fed
Pumice breccia D2-3 <i>Locality: G-east</i>	Very thick (up to 7 m); overall reversely graded and stratified into 5 well-preserved 1–2.5 m thick, normally or reversely graded beds separated by weak bed boundaries. Bed boundaries become less distinct upwards in the unit. Conformable with D2-2, in gradational to sharp contact. Gradational contacts are shown by decrease in size and abundance of major clasts of D2-2 in lower beds of D2-3. Coarse white pumice clasts at top of unit are aligned NE-SW. Locally, unit D2-3 can be found as a 1-m-thick lense below unit D2-2	Average grain size 0.2–60 cm; max. 120 cm Dominated by angular white pumice (mostly 70–95 vol%), grey andesite (mostly <30 vol%) and crystal fragment. Minor hydrothermally altered volcanic clasts and white aplyric pumice. D2-3a, b are rich in grey andesite and hydrothermally altered volcanic clasts (30–50 vol%). The base of bed D2-3b contains abundant coarse white pumice clasts as well as grey andesite clasts. Abundance of grey andesite clasts diminishes progressively in D2-3c–e (60 to <20 vol% upwards). Outsized grey andesite (3.5 m) with white pumice (30 cm) in bed D2-3e; hydrothermally altered pumice breccia (1 and >3 m) in various places in base to middle of unit D2-3	
Pumice breccia D2-3 <i>Locality: G-east</i>	Medium thick to very thick (up to 1 m), stratified. Basal contact sharp and discordant with D1. Locality G-west: medium bedded, normally graded; locality H: thickly bedded, normally graded; locality I: the 1-m-thick, reversely graded bed; lenses of coarse white pumice clasts at top	Average grain size 0.2–60 cm Mostly angular white pumice (>80 vol% of the clasts), with sub-dominant grey andesite, crystal fragment; rare outsized hydrothermally altered volcanic clasts (up to 60 cm) and white aplyric pumice clasts. Average grain size 0.2–1 cm	
Planar-stratified pumice breccia D2-4 <i>Localities: G, H</i>	Medium to thick, stratified, reversely to normally graded or massive; laminated at top. Gradational basal contact with D2-3. Multiple parallel laminations occur in the top 10 cm of each of the two beds	Mostly white pumice (10 mm; up to 15 vol%) and common white aplyric pumice (platy shape, imbricated towards SW, up to 3 cm; up to 35 vol%), crystal fragment, grey andesite, hydrothermally altered volcanic clasts	Explosive eruption-fed
		Average grain size 0.2–80 cm; max. 5 cm	

Table 2 (continued)

Beds, occurrence	Bed characteristics	Clast characteristics	Origin
Fine pumice breccia D2-5 <i>Localities: G, H</i>	Very thick (<3 m), diffusely stratified, overall reversely graded bed. Sharp and conformable basal contacts. Diffuse lenses of coarse (up to 45 cm) white pumice clasts are common	Mostly angular white pumice (>80 vol%, mostly <2 mm; max. 5 cm) and crystal fragment; minor grey andesite (>10 vol%, up to 1 cm). Rare outsized grey andesite clasts (<1 vol%; 6–40 cm) and hydrothermally altered volcanic clasts (<1 vol%) are present Average grain size 0.2–6 cm; max. 50 cm	Explosive eruption-fed
Cross-bedded pumice breccia-conglomerate D2-6 and D2-8 <i>Localities: G, H, I, J</i>	Thin to very thick tabular and stratified units; cross-bedding in trough (several meters in wavelengths) that can be compound (i.e. internally cross-stratified) (McKee and Weir 1953; Allen 1963) and show opposite palaeo-flow directions (Fig. 1). The basal contacts of both units are sharp and commonly cut across stratification in the beds beneath	Mostly sub-angular to sub-rounded white pumice (10–60 vol%; up to 150 cm), sub-dominant grey andesite, hydrothermally altered volcanic clasts and crystal fragment (up to 20 vol%), minor white aphyric pumice Average grain size 0.2–3 cm; max. 150 cm	Resedimented and reworked
Planar-bedded pumice breccia D2-7 <i>Localities: G, H, I</i>	Very thin to very thick; planar-bedded, tabular to lenticular, massive, or reversely or normally graded. Planar cross beds attesting of traction currents commonly occur, and graded beds can be stratified at their top. Sharp basal contact, some scouring. Strong bimodality occurs in medium to very thick beds at localities H and I, with randomly distributed, very coarse white pumice clasts (up to 1 m) in a diffusely stratified matrix mostly composed of white pumice clasts	Mostly white pumice (>80 vol%) and sub-dominant hydrothermally altered volcanic clasts and crystal fragment (up to 20 vol%), grey andesite (<1 vol%), white aphyric pumice Average grain size 0.2–1.6 cm; max. 100 cm	Explosive eruption-fed
Dogashima 3			
Weakly stratified andesite breccia D3 <i>Localities: C, I, J</i>	Extremely thick and clast-supported. Weakly stratified to massive, with disorganised, weakly stratified pumiceous matrix. Minimum volume estimated at $2 \times 10^6 \text{ m}^3$	Overall monomictic with coarsely porphyritic andesite; minor white pumice and hydrothermally altered volcanic clasts at base Average grain size is 20–50 cm; max. 100 cm	Resedimentation from effusive eruption

Fig. 8 Facies in Dogashima 1. **a** Top of the reversely graded pumice breccia (D1-5), locality E. Margins of the coarse white pumice clasts are very irregular and have been quenched; cauliflower textures occur in some clasts (*left arrow*). Image has been darkened to increase contrast. **b** Reversely graded pumice breccia (D1-2), locality B, with coarse white pumice clasts (*blue arrow*). Unit D1-2 has a discordant contact with overlying polymictic volcanic breccia (D1-3 and D1-8). D1-3 and D1-8 include similar coarse white pumice clasts. **c** Laminae of pyroxene crystal fragments and white pumice clasts in a stratified lens of planar-bedded pumice breccia (D1-1), locality D. **d** Cross-bedded pumice breccia (D1-1), locality B. Margins of coarse white pumice clasts (*blue arrows*) are interpreted to have been quenched. **e** Polymictic volcanic breccia (D1-3), locality D. The unit contains coarse white pumice clasts (beside notebook) derived from underlying pumice breccia units. **f** Polymictic volcanic breccia (D1-3), locality D. Grey scoria (*blue arrows*), white pumice clasts (*orange arrow*) and numerous types of hydrothermally altered volcanic clasts



Transport and depositional processes in Dogashima 2

Facies characteristics indicate that most units in Dogashima 2 were deposited from cohesionless, water-supported high-concentration density currents (e.g. Lowe 1982; Mulder and Alexander 2001; Talling et al. 2012). The units are laterally extensive, non- or weakly normally graded and clast-supported, and clay and silt matrix is very minor (<5 vol%). Many contacts are erosive, and oversized, dense clasts are common. This transport mode lies within the spectrum of ‘high-density turbidity currents’ of Lowe (1982). Similar density currents have also been named ‘high-density turbulent flows’ by Postma et al. (1988) and ‘concentrated density flows’ by Mulder and Alexander (2001). Other modes of subaqueous transport and deposition identified in Dogashima 2 are traction currents, rolling and sliding, suspension settling and turbidity currents (Table 2).

High-concentration density current deposits in Dogashima 2

Units D2-1 to D2-5 show an overall normal grading and a decrease in dense clasts upwards. The very thick beds of massive grey andesite breccia (D2-2) and pumice breccia (D2-3) at or near the base are tabular and laterally continuous and have gradational contacts at locations B, C and F (within the palaeo-channel). Units D2-2 to D2-3 have marked concentrations of dense clasts and thicken in topographic lows. Rounding of pumice clasts in D2-2 implies abrasion of these delicate clasts in the lower dense clast-dominated part of the current. The overall gradational contact between the andesite breccia D2-2 and pumice breccia D2-3 strongly suggests deposition from a single, sustained density current (e.g. Kokelaar et al. 2007). The high abundance of dense grey andesite clasts in D2-2 could have resulted from (1) preferential concentration of the densest components at the base of an

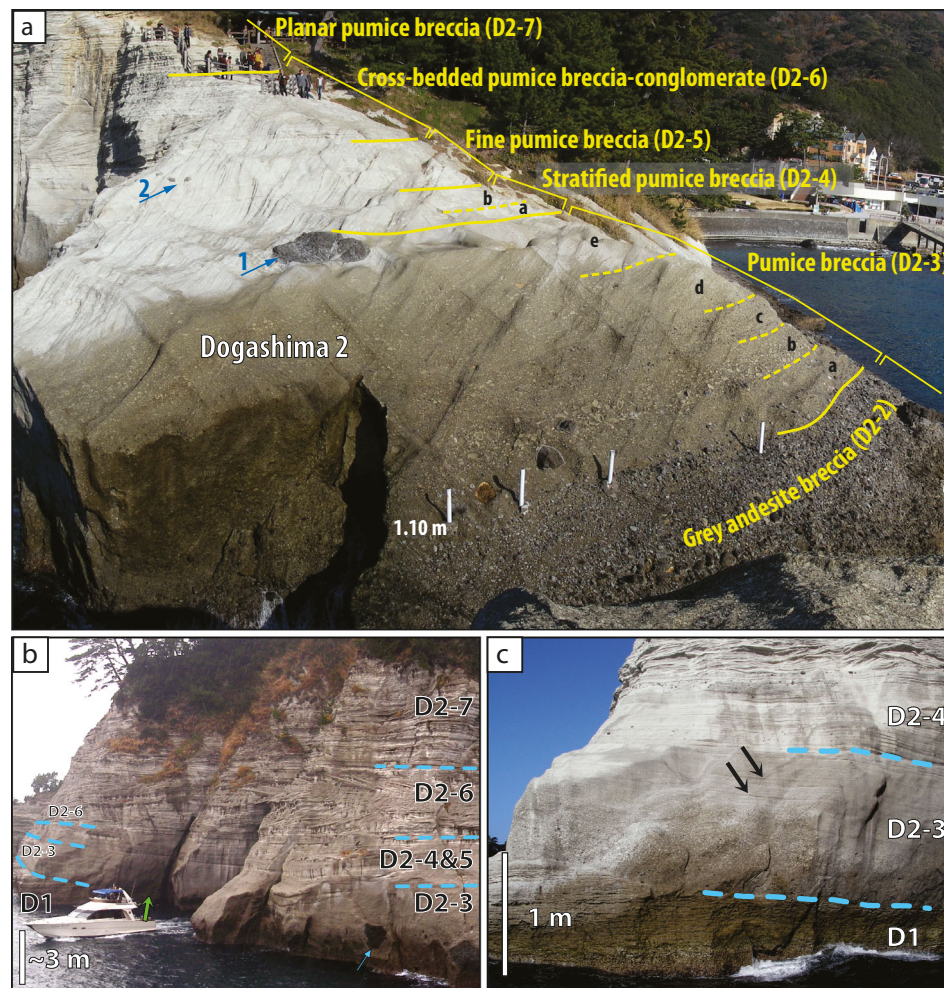


Fig. 9 Outcrops of Dogashima 2. **a** Locality G-east. Note the sharp boundary between the massive grey andesite breccia (D2-2) and the pumice breccia (D2-3), the locally graded units within the lower beds of the pumice breccia (beds a to e in D2-3), and the isolated grey andesite clast at the top (*arrow 1*) and in the fine pumice breccia (D2-5; *arrow 2*). **b** Lateral transition from the rim of the submarine channel (*right*) to overbank setting (*left*), locality G-west; this photo is a view just to left of picture **a**. Dogashima 1 (D1) is overlain by a relatively thin bed of pumice breccia (D2-3). D2-4 and D2-5 are stratified and partially eroded

in this section. The cross-bedded pumice breccia-conglomerate (D2-6) and planar-bedded pumice breccia (D2-7) overlie the entire section. Minor coarse grey andesite and hydrothermally altered volcanic clasts are present in D2-3 (*blue arrow*). *Green arrow* shows location of picture **c**. **c** Dogashima 2 at locality G-west, showing the rim of the submarine channel. Fine-grained facies of the pumice breccia (D2-3) overlies a disconformity with Dogashima 1 (D1). Note that unit D2-3 is relatively thin and stratified at the top (*arrows*); the basal polymictic volcanic breccia (D2-1) and massive grey andesite breccia (D2-2) beds are absent

initially heterogeneous current producing a complementary concentration of white pumice clasts higher up and/or (2) a temporal change in clast composition being supplied to the current from the source. Either way, clasts deposited from the current in the studied area changed from being mainly dense andesite to mainly white pumice. The basal unit D2-1 is dominated by dark andesite clasts derived from the underlying Matsuzaki Formation. These clasts were incorporated by shear-induced erosion in the lower part of the high-concentration density current that deposited units D2-2 and D2-3.

Very coarse (1–10 m) grey andesite clasts occur in local clusters in the middle and upper parts of the massive grey andesite breccia (D2-2) at all localities and define overall coarse-tail reverse grading. The biggest clasts were probably

big enough to locally modify the transporting current, favouring deposition of other coarse clasts. In addition, size segregation could have resulted from hindered settling during flowage, excluding some of the coarse clasts from the depositional boundary layer (e.g. Sohn and Chough 1993; Sohn 1997). Temporal increase in the size of clasts may have occurred in response to an increase in current velocity (waxing current) during progressive aggradation (e.g. Kneller and Branney 1995; Branney and Kokelaar 2002; Sumner et al. 2012), and/or ‘gliding’ of outsized clasts between a basal laminar inertia-flow and an upper turbulent flow may have been enhanced by flow confinement in channels (e.g. Postma et al. 1988). Alternatively, the supply of material at source may have become coarser through time, thus contributing to the reverse grading.

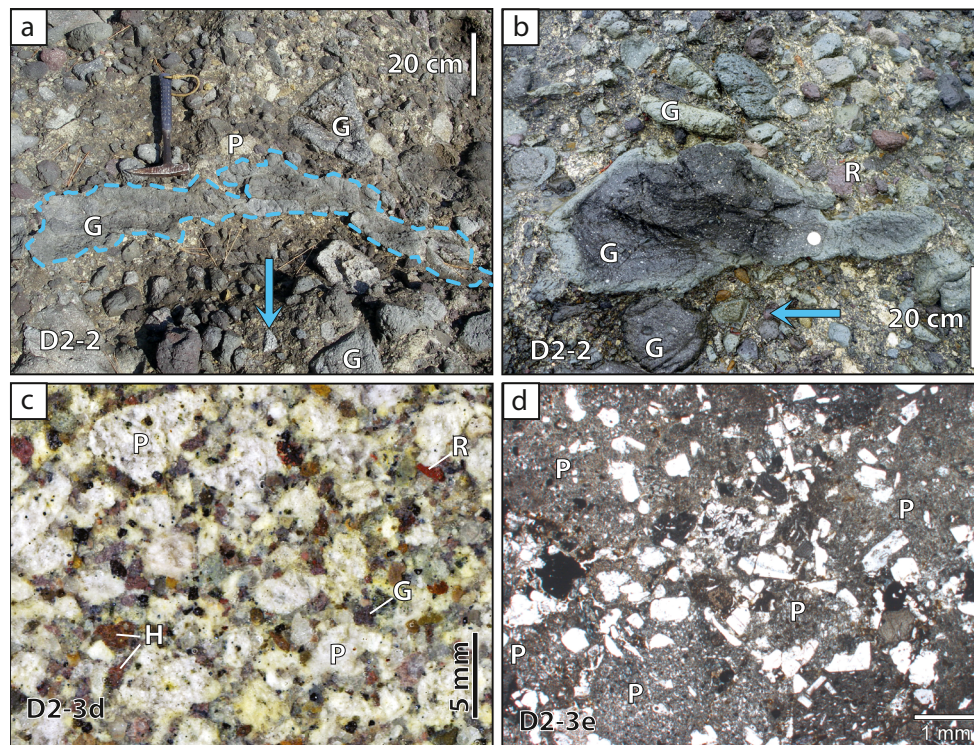


Fig. 10 **a, b** Elongate, fluidal-shape, grey andesite clasts in the massive grey andesite breccia (D2-2), amongst other angular clasts of grey andesite (*G*), white pumice (*P*) and red andesite (*R*); bird's-eye view, *arrow* indicates inferred flow direction from clast imbrication above in the stratigraphy, locality G-east. **c** Scan of a ground rock slab from the upper part of the pumice breccia (D2-3d) at locality G-east. The coarser white pumice clasts (*P*) are in hydraulic equivalence (Cashman and Fiske 1991)

with the finer dense clasts of grey andesite (*G*), red andesite (*R*) and hydrothermally altered volcanic clasts (*H*). Fine-grained components are crystal fragments. Note the absence of fine (<1/16 mm) components. **d** Photomicrograph of white pumice clasts (*P*) in a matrix chiefly made of crystal fragments (plagioclase, minor pyroxene), unit D2-3e; plane polarised light

The absence of stratification in units D2-2 and D2-3 in the centre of the channel indicates that the clast concentration was high enough to suppress turbulent segregation (e.g. Kokelaar et al. 2007; Talling et al. 2007). However, at the rim of the channel (locality G-east; Figs. 9a and 11), there is a sharp contact between units D2-2 and D2-3, at least five well-graded beds separated by weak bed boundaries are present in unit D2-3 and the top of unit D2-3 is hydraulically well-sorted and bimodal in clast componentry (Figs. 10 and 13). These features indicate local current unsteadiness and expansion and an increase in turbulence, which reduced the particle concentration and shear in the depositional boundary layer in the density current, promoting hydraulic sorting of the particles sedimenting from the current. Thus, the density current depositing D2-3 was affected by the uneven bathymetry. Most effects were focussed on the rim of the submarine channel, where it caused a flow transformation similar to a hydraulic jump (e.g. Komar 1971; Fisher 1983; Sumner et al. 2013). In addition, a pumice-rich lens is locally present below the dense clast-rich unit of D2-2 at locality G-east (Fig. 11), which suggests complex deposition and by-passing currents associated with uneven palaeo-bathymetry. This

part of the Dogashima Formation was previously interpreted by Cashman and Fiske (1991) to be the result of hydraulic sorting of clasts during fallout from a submarine eruption column and/or umbrella plume.

The increase in pumice clast size in the pumice breccia (unit D2-3) at localities C and G-east (Figs. 5 and 13) could be a depositional response to a flow surge (e.g. Lowe 1982; Mulder and Alexander 2001), or result from a change in the grain size of clasts supplied, or reflect palaeo-bathymetry effects, such as proposed for the underlying units. The strong preferred orientation of the coarse white pumice clasts at the top of unit D2-3e at locality G-east was probably caused by syn-depositional shear in the depositional boundary layer of the flow (e.g. Branney and Kokelaar 2002). Furthermore, the size of the extremely coarse (up to ~10 m), dense, grey andesite and hydrothermally altered volcanic clasts within the massive grey andesite breccia (unit D2-2) and pumice breccia (unit D2-3) implies a relatively short distance of transport. At locality G-east, the internal stratification and clast imbrication in the planar-stratified pumice breccia (D2-4) indicate the development of traction, unsteadiness or turbulence, all of which are typically associated with lower clast concentrations, and this unit may have been deposited from

the tail or waning phase of the current that deposited units D2-2 and D2-3. The fine pumice breccia unit (D2-5) is also weakly internally stratified, indicating current unsteadiness. Because of its similar componentry and stratigraphic proximity to units D2-3 and D2-4, it may be related to the density current that deposited the underlying units D2-1 to D2-4.

Traction currents in a submarine channel environment

The upper part of Dogashima 2 (units D2-6, D2-7 and D2-8) is planar and cross-stratified and very similar to the cross-bedded, planar-bedded and normally graded pumice breccia/sandstone (D1-1, D1-4, D1-7, D1-9 and D1-12) in Dogashima 1. In addition, some beds in these units contain sub-rounded white pumice clasts that indicate minor clast-clast interactions. Planar- and cross-stratification are commonly attributed to high-energy, semi-continuous traction currents that typically operate in above wave-base settings (e.g. DiMarco and Lowe 1989; Kano 1991; Allen et al. 1994; White et al. 2001). However, similar depositional structures can be formed on the deep sea floor around submarine volcanoes and in submarine canyons or channels, or on steep slopes (Wright 2001; Gardner 2010). Widespread siliciclastic dune fields in which single dunes have amplitudes up to several meters have been observed in submarine channels, and origins including tidal forces, internal waves and storm currents have been proposed (e.g. Valentine et al. 1984; Shanmugam 2008). Cross beds in D2-6 and D2-8 locally show opposite palaeo-current directions (Fig. 1; Table 3), which suggest complex sedimentation from up- and downslope currents, and/or reflection of currents on the margins of the channel, backsets and/or anti-dunes. A further consideration is that water-saturated, highly vesicular pumice clasts have a low specific gravity (~1.3; Allen et al. 2008) and are thus easily re-entrained compared to siliciclastic components of identical size (e.g. Manville et al. 2002). The angular to sub-rounded pumice clasts imply weak clast abrasion, thus does not match reworking in an above wave-base setting, where pumice clasts would be quickly rounded (White et al. 2001; Manville et al. 2002).

Other transport processes

The strongly bimodal grain size of pumice clasts versus matrix in some of the tabular, laterally extensive beds of unit D2-7 at localities H and I suggests that the coarse pumice clasts (~1 m) settled from suspension synchronously with finer grained clasts (<2 cm), waterlogging being delayed by their large size (e.g. Allen and McPhie 2009). The overall lateral continuity, local scouring, internal grading, relatively fine grain size and medium thickness of many beds in unit D2-7 are features

Fig. 11 a Reconstruction of the original geometry of the Dogashima Formation, which shows Dogashima 2 filling a submarine channel in Dogashima 1 (localities A to G-east). The submarine channel includes a palaeo-high at localities C to E and two palaeo-lows (localities A to B; F to G-east) carved into Dogashima 1. **b** Lateral changes in Dogashima 2 from localities G-west to G-east. A medium to thick, stratified bed of pumice breccia (D2-3) occurs at G-west (interpreted overbank setting; *left*) and overlies Dogashima 1 (D1) with a discordant contact. At G-east (interpreted submarine channel, *right*), thick beds of massive grey andesite breccia (D2-2) overlie D1 with a discordant contact. Locally, a lens of D2-3 occurs below D2-2 (*extreme right*). This lateral section is interpreted to represent the rim of the submarine channel carved in Dogashima 1. The logs are restricted to lower part of the cliff; all logs are ~5 m apart and start at sea level. The *red arrows* show the position of the 'submarine fallout layer' from Cashman and Fiske (1991); *person in yellow ellipse* for scale

consistent with lateral transport and deposition from sea floor-hugging, low-concentration turbidity currents (e.g. Shanmugam 2002; Piper and Normark 2009; Talling et al. 2012).

Eruption-fed versus resedimented facies

Clast source in the Dogashima Formation

The high abundance, high vesicularity, relatively fine size (mostly <10 cm) and overall angular shape of all types of pumice clasts in the Dogashima Formation imply that they are pyroclasts. The coarsest white pumice clasts (>30 cm) have remnants of quenched margins, implying quenching with seawater. The still-hot clasts of grey andesite, many with quenched margin remnants (Fig. 3b, c), and some with fluidal shape (Fig. 10a, b), indicate brecciation of a hot magma body (active lava, dome, cryptodome or other intrusion) that generated a coarse, dense, monomictic clast population. The significant volume of relatively fine, highly vesicular pumice clasts in pumice breccia D2-3 and the single thick emplacement unit in the lower part of Dogashima 2 (D2-1 to D2-3), together with crystal fragments in the matrix, indicate that the succession D2-1 to D2-3 was directly fed by an explosive eruption. Shard-rich siltstone units in Dogashima 1 (D1-6, D1-10) also strongly attest to a pyroclastic origin. In contrast, clasts derived from probable autobrecciation and/or quench fragmentation of lava include the coarsely porphyritic andesite clasts of Dogashima 3 and the dark andesite clasts resedimented from the Matsuzaki Formation.

Style of the eruption that produced Dogashima 2

The thickness and grain size of the D2-1 to D2-3 sequence indicate that this part likely represents the highest magnitude eruption amongst the units of the Dogashima Formation. As a

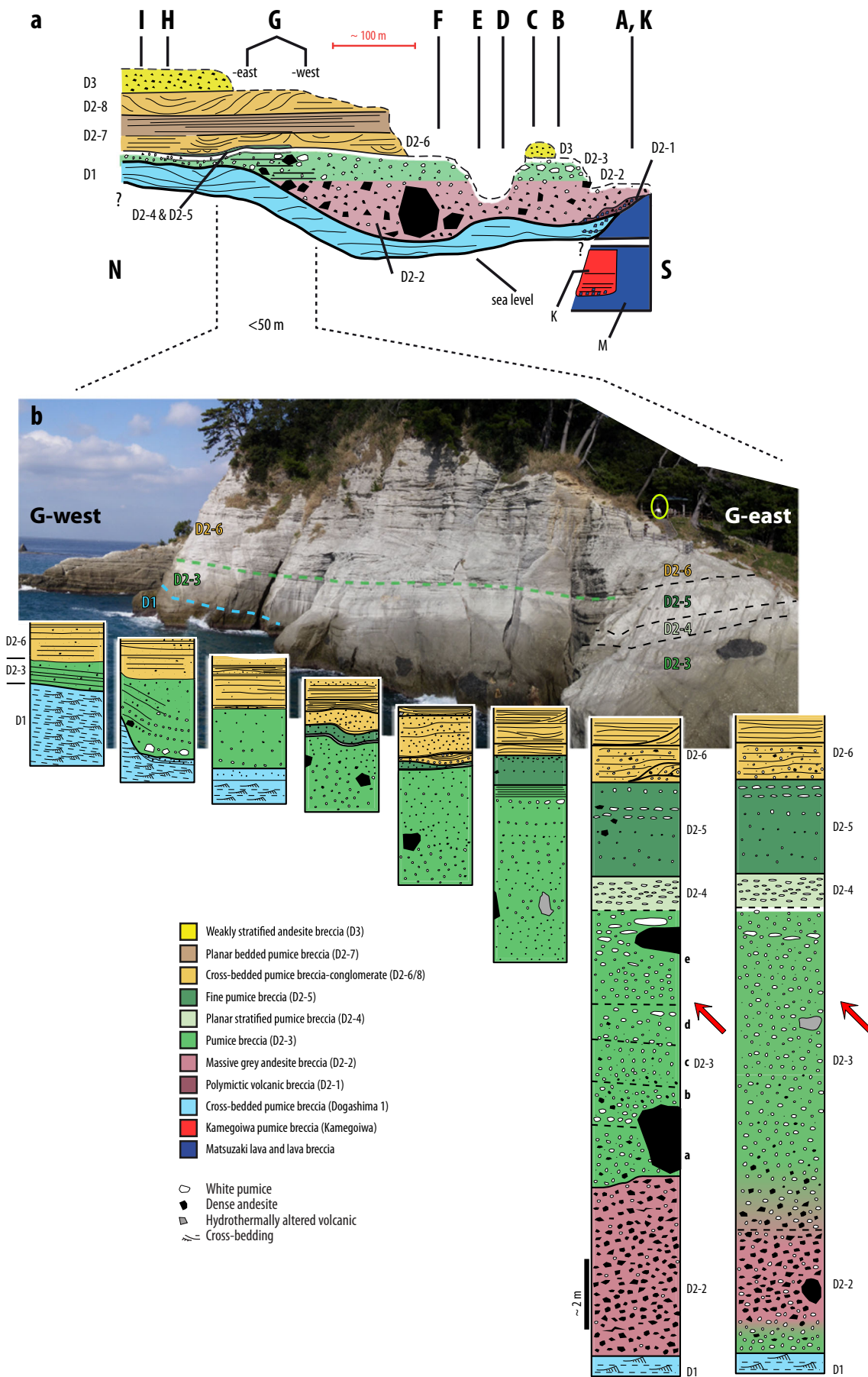
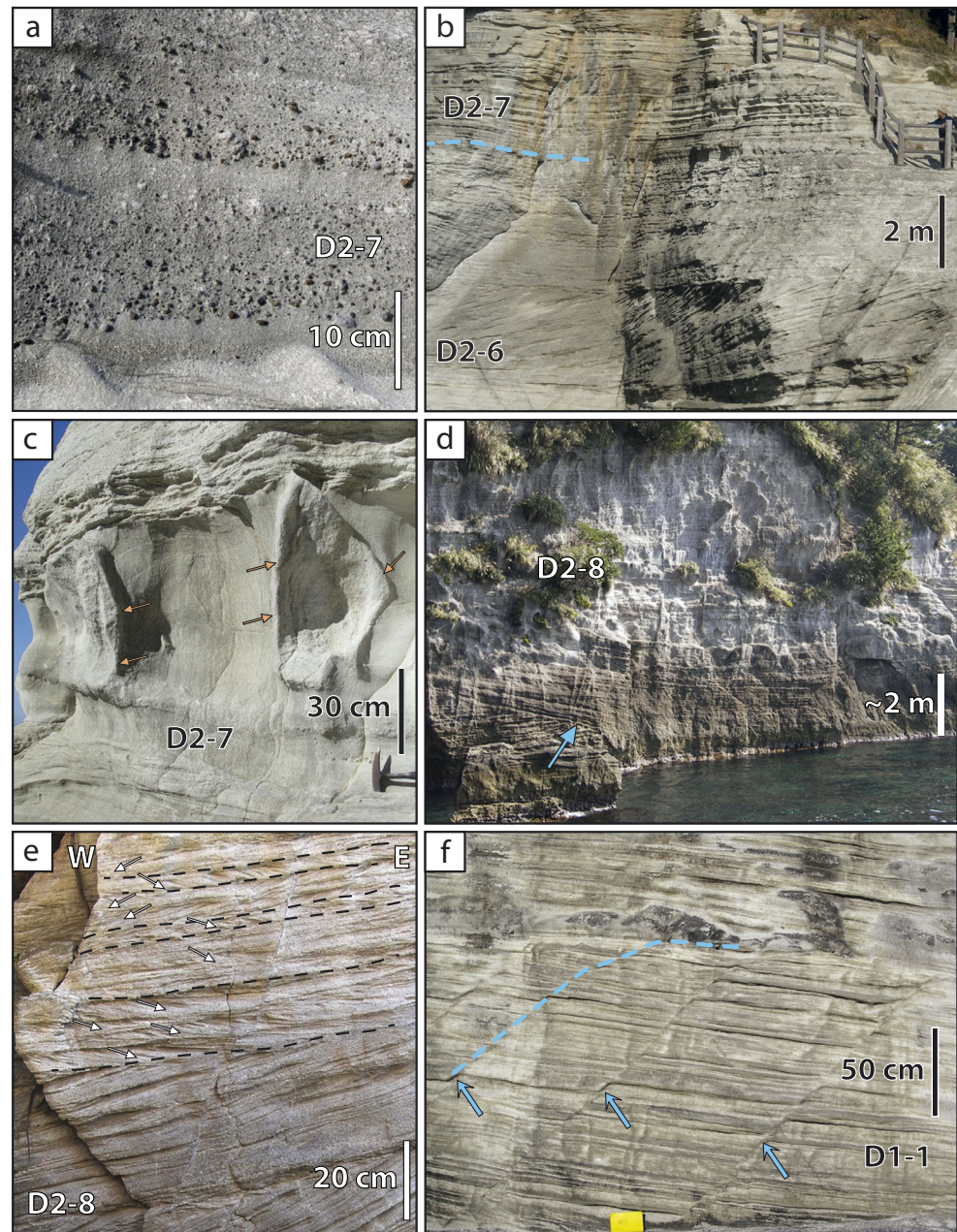


Fig. 12 **a** Normally graded beds in planar-bedded pumice breccia (D2-7), locality I. Grey andesite and hydrothermally altered volcanic clasts are abundant at the bases of the beds, whereas white pumice clasts are concentrated at the tops (density grading). **b** Large-scale planar and trough cross beds in cross-bedded pumice breccia-conglomerate (D2-6) and planar beds of the planar-bedded pumice breccia (D2-7), locality G-west. **c** Coarse pumice clasts (*orange arrows*) randomly distributed in a weakly stratified matrix of pumiceous sand, in planar-bedded pumice breccia (D2-7), locality I. **d** Large-scale trough cross beds (*blue arrow*) in cross-bedded pumice breccia-conglomerate (D2-8), locality H. **e** Small-scale compound (i.e. internally cross-stratified) cross beds in through cross-bedded pumice breccia-conglomerate (D2-8) at locality I. *Dashed lines* define beds with similar current direction; *white arrows* give the dominant bedding plane surface; *W* west, *E* east. **f** Syn-depositional normal faults (*blue line* and *arrows*; 75/110) cutting a very thick (>2 m) section of planar-bedded pumice breccia (D1-1) in Dogashima 1, locality D



result of confining pressure which reduces magmatic volatile exsolution, subaqueous magmatic volatile-driven explosive eruptions are inherently weaker than their subaerial counterparts (Head and Wilson 2003; Allen et al. 2008; Allen and McPhie 2009). In addition, rapid quenching and waterlogging of hot pumice clasts and condensation of steam promote eruption column collapse (Allen et al. 2008). The overall inferred transport in water-supported pumice-rich density currents, normal density grading through units D2-1 to D2-3 and the presence of suspension deposits (D2-7) show strong similarities with the products of ‘neptunian’ eruptions as defined by Allen and McPhie (2009). However, the high abundance of

originally hot dense grey andesite clasts in D2-1 (0–60 vol%), D2-2 (>90 vol%) and D2-3 (>20 vol%) indicates a close association with a still-hot, co-magmatic lava dome. In addition, the coarseness of the dense clasts within the D2-3 pumice breccia suggests that collapse and quenching occurred from relatively low heights within the eruption column and at only moderate eruption intensities, favouring transport in a single density-stratified density current. The presence of scattered large dense grey andesite clasts within D2-3 indicates the proximity of the Dogashima exposures to the vent and that destruction of the dome continued during deposition of the pumice-rich facies.

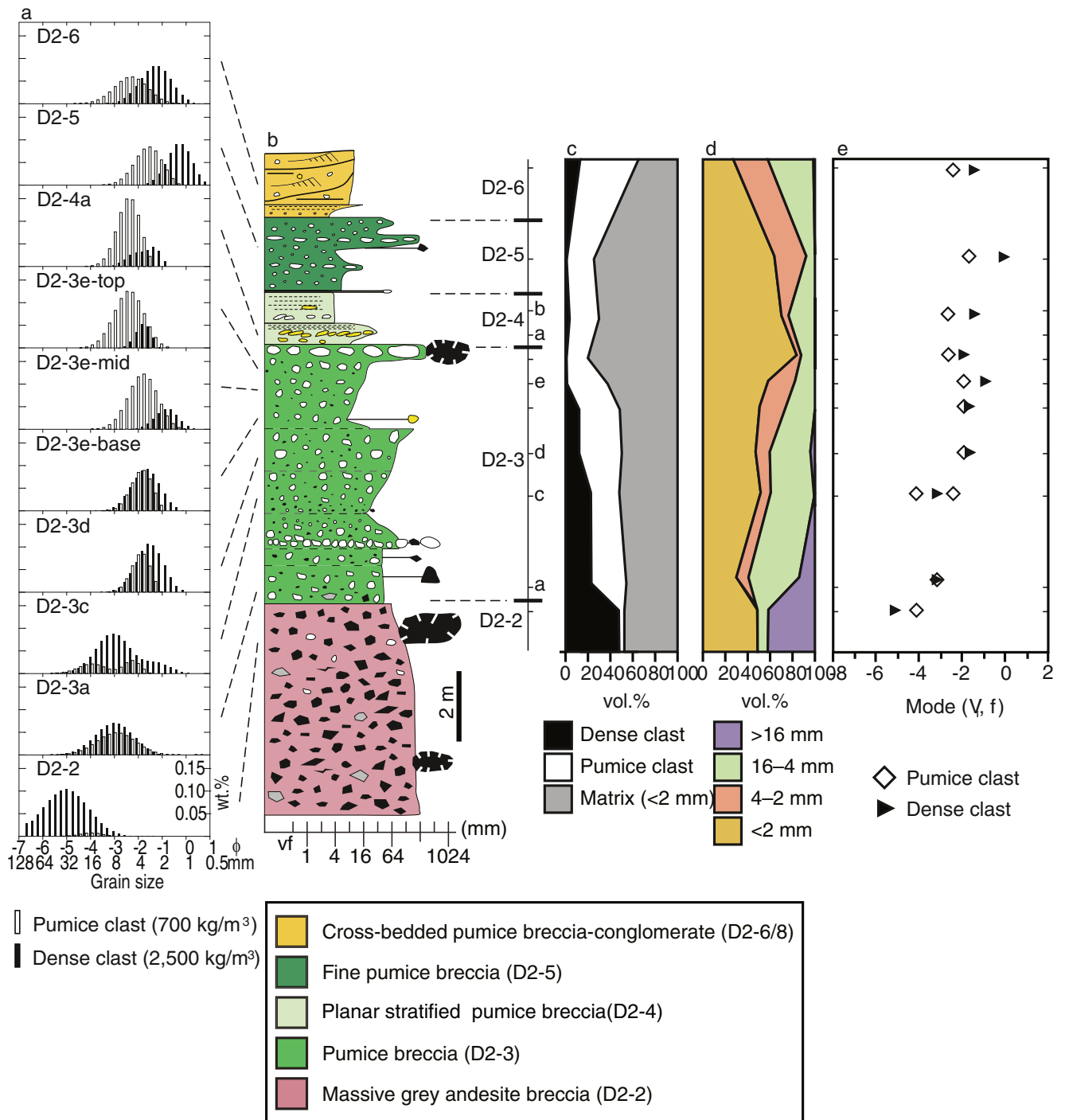


Fig. 13 Component volume and grain size distribution of white pumice and dense clasts (grey andesite and hydrothermally altered volcanic clasts) at locality G-east, in Dogashima 2. **a** Grain size distribution in weight percent for pumice and dense clasts, from image analysis and functional stereology (Jutzeler et al. 2012); bin at ¼ phi. **b** Stratigraphic

log of the basal part of Dogashima 2 at locality G-east. **c** Volume percent of clast types from image analysis. **d** Volume percent for size classes, from functional stereology data. **e** Volume modes for pumice and dense clasts from functional stereology data

Below wave-base, eruption-fed pyroclastic pumice-rich facies

The lower units (D2-2, D2-3) of Dogashima 2 have been previously interpreted as being the products of a pyroclastic eruption (Fiske 1969; Cashman and Fiske 1991; Tamura et al.

1991). The most direct evidence for an eruption-fed origin is that dense grey andesite clasts in D2-1 and D2-2 were hot on emplacement (Tamura et al. 1991). The presence of similar scattered coarse grey andesite clasts in the overall gradationally overlying pumice breccia (D2-3) implies that it is also

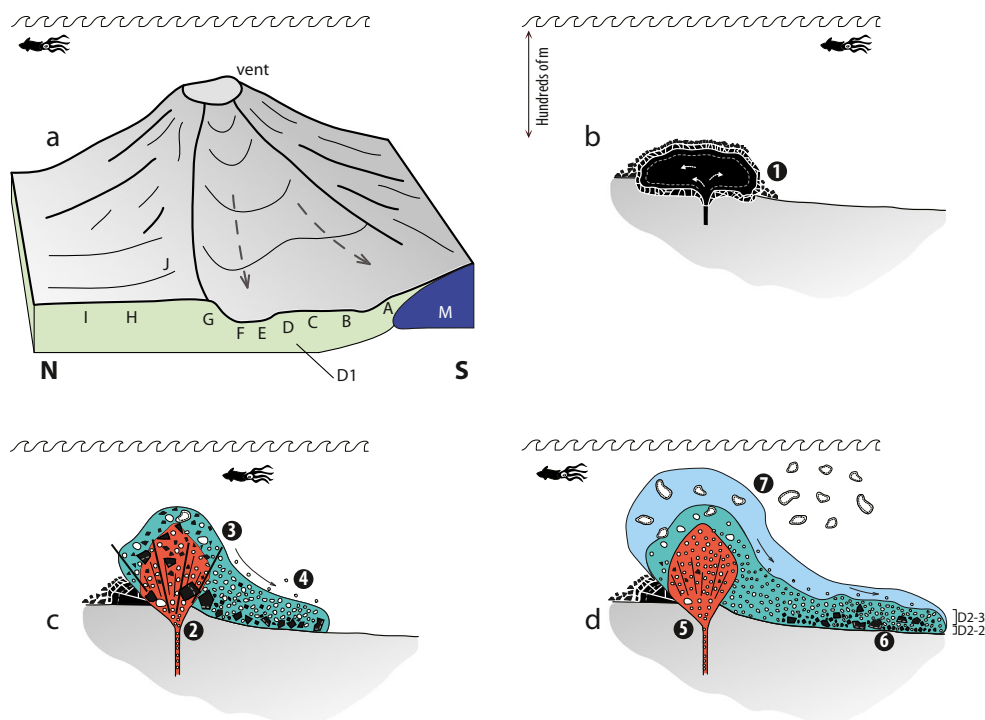


Fig. 14 Model involving destruction of a subaqueous dome by a magmatic volatile-driven explosive eruption; the vertical scale of the volcanic edifice is strongly exaggerated. **a** Geometry of the palaeo-channel just before deposition of Dogashima 2, N-S section. The palaeo-channel (sections A–G) and overbank locations (sections H–I) are at a lower elevation than the vent. Dogashima 1 (*green*). Palaeo-channel is centred on localities E, F and G, palaeo-high at C and D and palaeo-low between A and B. Matsuzaki Formation (*M*, *blue*) forms a palaeo-high to the south. **b** Effusive subaqueous eruption (1), producing an andesitic lava dome. **c** Destruction of the hot dome by a magmatic volatile-driven explosive eruption (2). Dense hot dome fragments (3) fall out rapidly. The eruption column collapses, producing (4) a water-supported,

subaqueous density current of grey andesite dome clasts and white pumice clasts (units D2-1 and D2-2). **d** Fewer dome clasts are available, and vesicular pumice clasts (5) become the dominant clast type in the collapsing eruption column (unit D2-3). Dense dome clasts are concentrated near the base of the water-supported high-concentration density current (6). Coarse pumice clasts are temporarily buoyant (7) and deposited from suspension later (unit D2-7). Waning stages of the eruption (D2-4, D2-5) and pumice resedimentation (D2-6 and D2-8) are not shown in cartoon. *Red* for explosive jet sustained by magmatic gases; *greenish blue* for water-supported region dominated by waterlogged pumice lapilli; *pale blue* for water-supported region with a lower concentration of finer grained clasts

Table 3 Bearing (true North) of long axes of elongate pumice clasts, interpreted to be deposited parallel to flow direction, in Dogashima 1 and 2. Flow direction inferred from clast imbrication. Dip direction of syn-depositional faults indicates palaeo-downslope direction

Unit	Locality	Long axis orientation (°)		Number of measures	Inferred flow orientation		Syn-depositional faults Dip/dip direction
		Primary	Secondary		Clast imbrication	Cross beds	
D1-1	B	265–285	215	7		E to W	
D1-1	D			>20			75/210
D1-3	D	235–245	225 and 275	18			
D1-8	D			3	E to W	E to W; W to E	
D2-3e	G-east	235–245		8			
D2-4	G-east	235–245		>10	E to W	E to W	
D2-6	G-west			>10		E to W; W to E	
D2-6	H	220		3			
D2-8	G-west			>10		E to W; W to E	
D2-8	I	245–265		6			
D2-8	I			>10	E to W		
D2-8	I			>10	E to W; W to E		
D2-8	J			>10	E to W; W to E		

eruption-fed. The characteristics of D2-3 can thus be taken to reliably indicate an explosive eruption-fed origin, confirming previous work aimed at identifying such facies (e.g. Cas and Wright 1991; McPhie et al. 1993; Kano et al. 1994, 1996; Kano 1996, 2003; Schneider et al. 2001; McPhie and Allen 2003). The characteristics of explosive eruption-fed facies include (1) very thick and extensive beds emplaced by density currents reflecting the rapid aggradation of a relatively large volume of pyroclasts; (2) being mainly composed of pyroclasts of uniform texture, mineralogy and composition; (3) the dominant clasts are moderately to highly vesicular, reflecting the role of magmatic volatiles in fragmentation; (4) the dominant clasts and overall grain size are relatively fine (coarse ash to lapilli); and (5) the dominant clasts are angular; some may have complete or partial quenched margins; and clast surfaces may be curvilinear and/or ragged.

The planar-stratified pumice breccia (D2-4) has a gradational lower contact with D2-3. This context implies that it was also eruption-fed even though it is only moderately thick and planar-stratified, both of which suggest that the clast supply and aggradation rates were less extreme than for D2-3. On the basis of context, the fine pumice breccia D2-5 is likely to be eruption-fed though probably related to a weaker eruption or eruption pulse, because it is planar-stratified and relatively fine and thin (Table 2), and the proportion of dense clasts is lower than in the units below.

Three units of Dogashima 1, the pumice breccia D1-2, D1-5 and D1-11, do not contain grey andesite clasts but are otherwise very similar to D2-3 and have characteristics that strongly suggest they were also explosive eruption-fed. They are unstratified, widespread and graded, implying deposition from subaqueous density currents, and mainly composed of fine, angular white pumice and crystal fragments.

By their thickness, lateral extent, grading and large volume of pyroclasts (including crystal fragments), the two Kamegoiwa breccias (K1-1 and K1-2) are also considered to be deposits from high-concentration eruption-fed density currents. In addition, loose substrate from the Matsuzaki Formation was picked up by the high-concentration density current, attesting to its ability to erode. Their stratified facies are interpreted to result from interaction with uneven palaeo-bathymetry, in a similar way to D2-3 at locality G-east.

Below wave-base, resedimented pyroclastic pumice-rich facies

Four units in Dogashima 2 (D2-4, D2-6, D2-7 and D2-8) and five units in Dogashima 1 (D1-1, D1-4, D1-7, D1-9 and D1-12) are mainly composed of highly vesicular white pumice clasts identical to those in the explosive eruption-fed pumice

breccia D2-3. These units are internally planar-bedded or cross-bedded, not laterally continuous, and individual beds are generally much less than 1 m thick. Importantly, the white pumice clasts are sub-rounded to rounded in many of these units. The dominance of relatively fine pumice clasts indicates a link to a subaqueous, magmatic volatile-driven explosive eruption, as for D2-3. However, in these nine units, rounding and sorting of pumice clasts, and the relatively thin, well-bedded depositional units indicate that aggradation was intermittent and involved relatively dilute, small-volume modes of transport, chiefly producing multiple, stratified, thin beds. These units are interpreted to be the products of downslope resedimentation from more proximal, primary pumice-rich facies (e.g. McPhie et al. 1993; Manville et al. 1998; Wright and Gamble 1999; Allen and Freundt 2006; Gardner 2010). The presence of resedimented facies interbedded with eruption-fed units throughout the Dogashima Formation indicates that syn- and/or post-eruption resedimentation was an important process. Interestingly, these units are not significantly more polymictic than eruption-fed facies, representing (surficial?) resedimentation of pumice-rich deposits from further upslope that had already been hydraulically sorted.

Comparison of resedimented and eruption-fed facies in the Dogashima Formation indicates that resedimentation involved small-volume, surficial, unconsolidated deposits and generated multiple sedimentation pulses, probably over large time scales, producing small-volume units bounded by sharp erosional surfaces. Given the long-time scales available for resedimentation, the total thickness (and volume) of resedimented units at the scale of an outcrop or at a locality can be equal to or larger than the actual underlying eruption-fed deposits. For example, the volume ratio of eruption-fed to resedimented deposits in D1 and D2 over the mapped area is at ca. 50:50.

Mass-wasting events

Partial destruction of an edifice is likely to remobilise clasts from various origins, histories and compositions, producing a polymictic, possibly multiple-bed deposit. Several causes can generate such collapse, such as mass-wasting events, or explosive eruptions. Volcanic breccia units (D1-3 and D1-8) include numerous clast types, and basal contacts scour the underlying beds of Dogashima 1. Both units are therefore interpreted as the products of mass-wasting events, or product of partial collapse of a volcanic cone.

The very coarse, overall monomictic, weakly stratified andesite breccia of Dogashima 3 is interpreted as resedimented autoclastic breccia, derived from collapse of a dome (or near-vent lava; Jutzeler 2012). The weakly stratified pumiceous sandstone matrix in Dogashima

3 is interpreted to have been deposited after the andesite clasts, from raining down and filtering of clasts brought by marine currents through the interstices between the clasts in the unconsolidated clast-supported breccia (e.g. Gifkins et al. 2002).

Eruption narrative

The Dogashima Formation is a combination of products from explosive eruptions, dome destruction and inter-eruptive resedimentation. From detailed facies analysis, we reconstruct the various eruption and transport processes involved in the accumulation of the volcanoclastic facies (Fig. 14).

Phase 1: explosive activity (Kamegoiwa)

Kamegoiwa pumice breccia (units K1-1 and K1-2) records the lowermost known part of the Dogashima Formation. The high abundance of highly vesicular, white aphyric pumice lapilli and crystal fragments records deposition of at least two high-concentration density currents derived from magmatic volatile-driven explosive eruptions. The magma composition being different from the other clasts of the Dogashima Formation, its magmatic source and vent are likely to be distinct from the overlying units. K1-2 is locally overlain (intruded?) by lavas from the Matsuzaki Formation. There is a stratigraphic gap (sea level, fault, intrusions) between outcrops of K1-2 and Dogashima 1.

Phase 2: intermittent explosive activity and resedimentation (Dogashima 1)

Dogashima 1 comprises three units (D1-2, D1-5 and D1-11) that record direct deposition from subaqueous, explosive eruption-fed density currents and two units (D1-6 and D1-10) that were deposited from suspension settling associated with explosive eruptions. These pyroclastic units are intercalated with seven units (D1-1, D1-3, D1-4, D1-7, D1-8, D1-9, D1-12; Table 2; Fig. 5) that are resedimented equivalents of the eruption-fed units. The eruption-fed units are relatively thin (<3 m) and composed of highly vesicular pumice lapilli, implying that the eruptions were magmatic volatile-driven though relatively small volume. There is no evidence for the presence of a dome at the vent during this phase. Phase 2 is interpreted to record earlier (precursory?) explosive activity to the climactic eruption recorded by D2-3.

Phase 3: effusive eruption (D2-1, D2-2)

The basal units of Dogashima 2 overlie an erosional discontinuity interpreted to be submarine channel in the beds of Dogashima 1. The two lowest units, D2-1 and D2-2, are

breccias composed of dense grey andesite clasts that were hot at deposition. These clasts must have been derived from an active lava dome (or near-vent lava flow) that had a volume in the order of $\sim 1 \times 10^6 \text{ m}^3$ (Fig. 14b; Jutzeler 2012). The grey andesite clasts have a slightly less evolved composition than the white pumice clasts in the eruption-fed units of Dogashima 1, but the compositions are similar enough to infer that they came from closely related magmas at the same volcano and probably the same vent. The grey andesite clasts in Dogashima 2 are dense, non-vesicular and massive (i.e. no flow bands). A white pumice clast containing a blob of dense grey andesite in D2-3e suggests very minor magma mingling in a shared conduit/vent.

Subaqueous domes and crypto-domes commonly have a poorly vesicular core and a rim that is flow-banded and/or pumiceous (e.g. Gifkins et al. 2002; Goto and Tsuchiya 2004; Allen et al. 2010) although the volume of flow-banded and vesicular facies can be minor in comparison to the massive, poorly vesicular core (Goto and Tsuchiya 2004). The absence of vesicles in the grey andesite clasts suggests that the source andesite had a low volatile content. Another possibility is that the clasts came from a cryptodome sufficiently deep to prevent vesiculation. If the grey andesite clasts were derived from an intrusion, then non-juvenile clasts representing the cover ought to be present in the breccias. However, <5 vol% of hydrothermally altered volcanic clasts occur in D2-2 suggesting that a cryptodome source is unlikely. Therefore, we favour the interpretation that a gas-poor, andesitic lava dome was extruded on the same volcano that generated the eruption-fed pumice breccia units in phase 2 and was subsequently destroyed while still hot. Dome growth probably occurred during the pause in aggradation recorded by the unconformity at the top of Dogashima 1, although no deposit at Dogashima attests of this growth.

Phase 4: climactic explosive pumice-forming eruption (D2-2 to D2-5)

Units D2-3 to D2-5 are thick and dominantly composed of andesitic pumice clasts and crystal fragments generated by a small-volume magmatic volatile-driven explosive eruption. This eruption was initially dome-seated and destroyed the active lava dome (Fig. 14c). The sequence D2-1 to D2-4 shows overall normal grading in clast density and gradational contacts, reflecting continuous deposition from a single density current composed of juvenile pumice clasts and hot-dome-derived (Tamura et al. 1991) dense clasts (Fig. 14c, d). The componentry in D2-2 and D2-3 implies that the density current was first overloaded with hot dense grey andesite clasts but gradually changed to be dominated by white pumice clasts (Fig. 14c, d). However, the current was heterogeneous enough to locally deposit a lens of pumice breccia below grey andesite breccia (Fig. 11). The very good hydraulic sorting of

waterlogged white pumice clasts and dense clasts in D2-3 at the margins of the channel is the result of local increase in turbulence and flow expansion of the high-concentration density current. The planar-stratified pumice breccia (D2-4) overlying D2-3 was probably deposited from the less-concentrated waning tail of the current (Fig. 14d). The fine pumice breccia (D2-5) may have been produced by an eruption similar to that responsible for D2-3, but less intense, generating a weaker and unsteady density current.

Phase 5: resedimentation and suspension settling (D2-6 and D2-8)

The units of cross-bedded pumice breccia-conglomerate (D2-6 and D2-8) record downslope resedimentation of the freshly erupted pyroclasts from a more proximal site by strong currents in a submarine channel. The laterally continuous bed of planar-bedded pumice breccia (D2-7) that is part of this sequence comprises coarse white pumice clasts and ash settled from suspension. The pyroclasts were either erupted at the same time as the white pumice clasts of D2-3, or from a subsequent eruption.

Phase 6: effusive eruption (Dogashima 3)

The andesite clasts in the weakly stratified, coarsely porphyritic andesite breccia of Dogashima 3 have a distinctive composition and record extrusion and disintegration of a new lava dome, such as by lava flow front or dome collapse. The lack of vesicular clasts suggests that the magma was relatively volatile-poor. The pumiceous sand that forms the matrix of Dogashima 3 was probably derived from the pumice-rich products of the main explosive eruption of D2-3, which were subsequently resedimented.

Discussion

A submarine fall deposit in the Dogashima Formation?

Cashman and Fiske (1991) interpreted the pumice breccia at locality G-east (beds D2-3d and D2-3e in this study) to be a submarine fall deposit from a submarine eruption, drawing attention in particular to the good hydraulic sorting of white pumice and dense grey andesite clasts (Figs. 10c, d and 13). However, the hydraulically well-sorted facies in beds D2-3d and D2-3e is only present at locality G-east; it can be traced for no more than 10 m laterally over the hundreds of meters of exposures. D2-3 pinches out at the rim of the palaeo-channel and in the overbank (localities G-west, I and J; Figs. 9 and 11), where it is almost exclusively composed of pumice lapilli and feldspar crystal fragments. In the channel (localities A–F;

Figs. 1 and 5), unit D2-3 is very thick, tabular and massive; contains minor lenses of coarse pumice clasts; and has a gradational lower contact with the massive grey andesite breccia (D2-2), and no coexistence of pumice and density-equivalent dense clasts could be detected.

Subaqueous fall deposits should mimic some of the major characteristics of fall deposits from subaerial explosive eruption columns (e.g. Pyle 1989), including non-erosive lower contacts, lateral continuity over substantial distances and systematic thickness and grain size changes with distance from source. None of these characteristics are displayed by either the interval of the submarine fall deposit of Cashman and Fiske (1991) (D2-3d, D2-3e in this study) or by the gradationally enclosing D2-1 to D2-3 succession. In addition, the high concentration of pyroclasts present in a submarine eruption column (such as for Dogashima 2) will promote formation of vertical density currents (Manville and Wilson 2004). In vertical density currents, clast velocity and sorting conditions are strongly different in comparison to low clast concentration, such as used for the experiments by Cashman and Fiske (1991).

This study shows that D2-3, and in fact much of Dogashima 2, was deposited from sea floor-hugging, eruption-fed density currents in a submarine channel setting. Locality G-east occurs on the rim of the submarine channel that lies between localities A and G-east. The uneven palaeo-bathymetry may have caused current unsteadiness and expansion that increased turbulence, in a similar way to a hydraulic jump (e.g. Komar 1971; Fisher 1983; Sumner et al. 2013), depositing the locally stratified and hydraulically sorted facies studied by Cashman and Fiske (1991).

Production and deposition of shards

The very low abundance of juvenile glass shards in eruption-fed facies of the Dogashima Formation may be characteristic of the products of subaqueous explosive eruptions where the column remains underwater (Allen et al. 2008; Allen and McPhie 2009) and subsequent pyroclast transport occurs in water-supported density currents. A fines-poor character could be due to a combination of factors such as (1) reduced explosivity of subaqueous explosive eruptions under confining pressure compared to their subaerial counterparts (Head and Wilson 2003; Allen et al. 2008); (2) reduced production of shards through clast-clast interactions in the eruption column and during outflow because of the higher viscosity of water compared to air (e.g. White 2000); and (3) segregation and advection of fine buoyant shards with low settling velocities into buoyant plumes of seawater heated by the eruption and/or during lateral transport (e.g. Cantelli et al. 2008) and deposition elsewhere.

Water-settled facies in the Dogashima Formation

Shard-rich siltstone units (D1-6 and D1-10) and a bed in the planar-bedded pumice breccia (unit D2-7) extend tens of meters laterally and best exemplify the kind of water-settled fall facies generated by subaqueous magmatic volatile-driven explosive eruptions. D1-6 and the bed in D2-7 contain very coarse (~1 m) white pumice clasts. The coarse pumice clasts in these units probably cooled slowly as a result of their size and remained buoyant until sufficiently waterlogged to sink, along with shards which have slow settling velocities (e.g. suspension deposits; Allen and McPhie 2009). The shard-rich units D1-10 and D2-7 do not directly overlie eruption-fed density current deposits; however, the distinctive componentry, bimodal grain size (shards versus coarse white pumice clasts) and lithofacies characteristics suggest that they are suspension deposits generated by subaqueous explosive eruptions; any related density currents are inferred to have left their deposits elsewhere. The bimodal (ash and crystals versus coarse white pumice clasts) bed in D2-7 could be related to the explosive eruption that formed units D2-1 to D2-5. If correct, the presence of unit D2-7 at the same site as the density current deposits D2-1 to D2-5 suggests that deposition of the entire Dogashima 2 sequence was relatively rapid and broadly syn-eruptive. However, the presence of cross-bedded pumice breccia-conglomerate (unit D2-6) immediately beneath unit D2-7 indicates a time break in the eruptive activity after deposition of D2-5. Therefore, D2-7 may be related to another subaqueous explosive eruption that did not produce a density current deposit at Dogashima (similar to D1-10).

Conclusions

The Pliocene Dogashima Formation (4.55 ± 0.87 Ma; Izu Peninsula, Japan) records subaqueous effusive and magmatic volatile-driven explosive volcanic activity and inter-eruptive resedimentation in a below wave-base, open-marine setting. The similar bulk compositions, mineralogy and feldspar compositions of the white pumice and grey andesite clasts in D1 and D2 in the Dogashima Formation suggest that these components were co-magmatic and erupted from the same or closely adjacent subaqueous vent(s).

Thermoremanent temperatures (Tamura et al. 1991) and well-preserved quenched margins and fluidal textures on dense grey andesite clasts in the lower part of Dogashima 2 show that these clasts were hot when deposited. The high abundance of the dense grey andesite clasts in the lowermost units of Dogashima 2, D1-1 and D2-2, implies that these units record destruction of an active submarine andesite dome. Pumice breccia D2-3 also contains the coarse, originally hot, grey andesite clasts though the dominant components are highly

vesicular andesitic pumice. We infer that dome destruction involved a magmatic volatile-driven, subaqueous, explosive eruption. The explosive eruption fed a sea floor-hugging water-supported density current that changed in composition from being dense andesite-dominated (D2-1, D2-2) to being andesitic pumice-dominated (D2-3) and from being highly concentrated (D2-1, D2-2, D2-3) to being more diluted (D2-4, D2-5).

Explosive eruption-fed, water-supported, high-concentration density current deposits are recognised by their occurrence in thick and extensive depositional units that were aggraded rapidly and are dominated by an angular, relatively fine (coarse ash to lapilli), highly vesicular pyroclasts of uniform texture; massive to graded units are common, and stratification may be present, depending partly on substrate morphology. Local incorporation of the loose substrate, erosional basal contacts and channel-filling context are additional indicators of deposition from sea floor-hugging high-concentration density currents. Other units in the Dogashima Formation (e.g. K1-1, K1-2, D1-2, D1-5, D1-11), and indeed in subaqueous successions elsewhere that show similar facies characteristics but lack the originally hot clasts, are also likely to be explosive eruption-fed subaqueous density current deposits. Coarse pumice clasts and ash in overlying planar-bedded pumice breccia (D2-7) are also interpreted to have an explosive eruption-fed origin but one involving settling of pyroclasts from suspension rather than suspension from a density current.

Relatively well-sorted, planar-bedded and cross-bedded facies between the eruption-fed units are also composed of highly vesicular pumice clasts but contain sub-rounded pumice clasts. The weak rounding of clasts, relatively thin units and well-bedded character indicate that these facies were resedimented from more proximal, but below wave-base locations. Resedimentation is a predictable consequence of the presence of a large volume of relatively fine, low-density pyroclasts on the sea floor.

Dogashima 2 accumulated in a broad (650×15 m) submarine channel. The internal stratification and good hydraulic sorting within the pumice breccia (D2-3) at the rim of the palaeo-channel (locality G-east) are attributed to local current expansion and an increase in unsteadiness and turbulence from wall effects affecting the density current and are not indicative of a submarine fall deposit *sensu* Cashman and Fiske (1991). Well-developed planar- and cross-stratification suggests that traction currents operated within the submarine channel.

Acknowledgments This study was supported by the Australian Research Council and is part of the PhD thesis of M.J. We thank R. Fiske, M. Ort, J.D.L. White and S.M. Gordee for helpful discussions on this paper. V. Manville, K. Kano, R.A.F. Cas and R. Fiske thoroughly reviewed an earlier manuscript. K.-I. Kano is thanked for his help with the fieldwork in Japan; J.M. and M.J. are grateful to the Shimoda Marine Research Center (Japan) for accommodation. S. Meffre, K. Goemann and P. Robinson conducted part of the chemical and geochronological analyses.

References

- Allen JRL (1963) The classification of cross-stratified units, with notes on their origin. *Sedimentology* 2:93–114
- Allen SR, Freundt A (2006) Resedimentation of cold pumiceous ignimbrite into water: facies transformations simulated in flume experiments. *Sedimentology* 53:717–734. doi:10.1111/j.1365-3091.2006.00790.x
- Allen SR, McPhie J (2000) Water-settling and resedimentation of submarine rhyolitic pumice at Yali, eastern Aegean, Greece. *J Volcanol Geotherm Res* 95:285–307
- Allen SR, McPhie J (2009) Products of neptunian eruptions. *Geology* 37:639–642. doi:10.1130/G30007A.1
- Allen JRL, Friend PF, Lloyd A, Wells H (1994) Morphodynamics of intertidal dunes: a year-long study at Lifeboat Station Bank, Wells-next-the-Sea, Eastern England. *Philos Trans R Soc A* 347:291–344
- Allen SR, Fiske RS, Cashman KV (2008) Quenching of steam-charged pumice; implications for submarine pyroclastic volcanism. *Earth Planet Sci Lett* 274:40–49. doi:10.1016/j.epsl.2008.06.050
- Allen SR, Fiske RS, Tamura Y (2010) Effects of water depth on pumice formation in submarine domes at Sumisu, Izu-Bonin Arc, western Pacific. *Geology* 38:391–394. doi:10.1130/G30500.1
- Branney MJ, Kokelaar P (2002) Pyroclastic density currents and the sedimentation of ignimbrites. Geological Society, London
- Cantelli A, Johnson S, White JDL, Parker G (2008) Sediment sorting in the deposits of turbidity currents created by experimental modeling of explosive subaqueous eruptions. *J Geol* 116:76–93
- Carey RJ, Wysoczanski R, Wunderman R, Jutzeler M (2014) Discovery of the largest historic silicic submarine eruption. *Eos Trans AGU* 95:157–159. doi:10.1002/2014EO190001
- Cas RAF, Wright JV (1991) Subaqueous pyroclastic flows and ignimbrites: an assessment. *Bull Volcanol* 53:357–380. doi:10.1007/BF00280227
- Cas RAF, Allen RL, Bull SW, Clifford BA, Wright JV (1990) Subaqueous, rhyolitic dome-top tuff cones: a model based on the Devonian Bunga Beds, southeastern Australia and a modern analogue. *Bull Volcanol* 52:159–174
- Cashman KV, Fiske RS (1991) Fallout of pyroclastic debris from submarine volcanic eruptions. *Science* 253:275–280. doi:10.1126/science.253.5017.275
- DiMarco MJ, Lowe DR (1989) Shallow-water volcanoclastic deposition in the Early Archean Panorama Formation, Warrawoona Group, eastern Pilbara Block, Western Australia. *Sediment Geol* 64:43–63
- Fisher RV (1961) Proposed classification of volcanoclastic sediments and rocks. *Geol Soc Am Bull* 72:1409–1414. doi:10.1130/0016-7606(1961)72[1409:PCOVSA]2.0.CO;2
- Fisher RV (1983) Flow transformations in sediment gravity flows. *Geology* 11:273–274
- Fiske RS (1969) Recognition and significance of pumice in marine pyroclastic rocks. *Geol Soc Am Bull* 80:1–8. doi:10.1130/0016-7606(1969)80[1:RASOPI]2.0.CO;2
- Fiske RS, Matsuda T (1964) Submarine equivalents of ash flows in the Tokiwa Formation, Japan. *Am J Sci* 262:76–106
- Fiske RS, Cashman KV, Shibata A, Watanabe K (1998) Tephra dispersal from Myojinsho, Japan, during its shallow submarine eruption of 1952–1953. *Bull Volcanol* 59:262–275. doi:10.1007/s004450050190
- Fiske RS, Naka J, Iizasa K, Yuasa M, Klaus A (2001) Submarine silicic caldera at the front of the Izu-Bonin Arc, Japan; voluminous seafloor eruptions of rhyolite pumice. *Geol Soc Am Bull* 113:813–824
- Gardner JV (2010) The West Mariana Ridge, western Pacific Ocean: geomorphology and processes from new multibeam data. *Geol Soc Am Bull* 122:1378–1388. doi:10.1130/B30149.1
- Geological Survey of Japan (2010) Seamless digital geological map of Japan 1:200,000. In: AIST GSJ (ed) Research information database DB084. Geol. Surv. Jpn. AIST, Japan
- Gifkins CC, McPhie J, Allen RL (2002) Pumiceous rhyolitic peperite in ancient submarine volcanic successions. *J Volcanol Geotherm Res* 114:181–203. doi:10.1016/S0377-0273(01)00284-0
- Gordec SM, McPhie J, Allen SR (2008) Facies mapping of volcanic and sedimentary facies of a partly extrusive submarine cryptodome, Mio-Pliocene Shirahama Group, Izu Peninsula, Japan. In: IAVCEI General Assembly, Iceland
- Goto Y, Tsuchiya N (2004) Morphology and growth style of a Miocene submarine dacite lava dome at Atsumi, northeast Japan. *J Volcanol Geotherm Res* 134:255–275. doi:10.1016/j.jvolgeores.2004.03.015
- Head JW, Wilson L (2003) Deep submarine pyroclastic eruptions: theory and predicted landforms and deposits. *J Volcanol Geotherm Res* 121:155–193
- Huchon P, Kitazato H (1984) Collision of the Izu Block with central Japan during the quaternary and geological evolution of the Ashigara area. *Tectonophysics* 110:201–210
- Ibaraki M (1981) Geologic ages of “Lepidocyclina” and Miogypsina horizons in Japan as determined by planktonic foraminifera. In: Ikebe N, Chiji M, Tsuchi R, Morozumi Y, Kawata T (eds) IGCP-114; International workshop on Pacific Neogene biostratigraphy; 6th international working group meeting, Osaka, Japan, Nov 25–29, 1981. Osaka Mus. Nat. Hist., Osaka, Japan (JPN), p 118–119
- Ingram RL (1954) Terminology for the thickness of stratification and parting units in sedimentary rocks. *Geol Soc Am Bull* 65:937–938. doi:10.1130/0016-7606(1954)65[937:TFTTOS]2.0.CO;2
- Jutzeler M (2012) Characteristics and origin of subaqueous pumice-rich pyroclastic facies: Ohanapeosh Formation (USA) and Dogashima Formation (Japan). Ph.D. thesis, University of Tasmania, Hobart, Australia, Hobart, Australia
- Jutzeler M, Proussevitch AA, Allen SR (2012) Grain-size distribution of volcanoclastic rocks 1: a new technique based on functional stereology. *J Volcanol Geotherm Res* 239–240:1–11. doi:10.1016/j.jvolgeores.2012.05.013
- Jutzeler M, McPhie J, Allen SR (2014a) Facies architecture of a continental, below-wave-base volcanoclastic basin: the Ohanapeosh Formation, Ancestral Cascades arc (Washington, USA). *Geol Soc Am Bull* 126:352–376. doi:10.1130/B30763.1
- Jutzeler M, Marsh R, Carey RJ, White JDL, Talling PJ, Karlstrom L (2014b) On the fate of pumice rafts formed during the 2012 Havre submarine eruption. *Nat Commun* 5:3660. doi:10.1038/ncomms4660
- Kano K-I (1983) Structures of submarine andesitic volcano—an example in the Neogene Shirahama group in the southern part of the Izu Peninsula, Japan. *Geosci Rep Shizuoka Univ* 8:9–37
- Kano K-I (1989) Interactions between andesitic magma and poorly consolidated sediments: examples in the Neogene Shirahama Group, South Izu, Japan. *J Volcanol Geotherm Res* 37:59–75
- Kano K (1991) Volcanoclastic sedimentation in a shallow-water marginal basin: the Early Miocene Koura Formation, SW Japan. *Sediment Geol* 74:309–321
- Kano K (1996) A Miocene coarse volcanoclastic mass-flow deposit in the Shimane Peninsula, SW Japan: product of a deep submarine eruption? *Bull Volcanol* 58:131–143. doi:10.1007/s004450050131
- Kano K (2003) Subaqueous pumice eruptions and their products; a review. In: White JDL, Smellie JL, Clague DA (eds) Explosive subaqueous volcanism. AGU, Washington, pp 213–230
- Kano K, Orton GJ, Kano T (1994) A hot Miocene subaqueous scoria-flow deposit in the Shimane Peninsula, SW Japan. *J Volcanol Geotherm Res* 60:1–14
- Kano K, Yamamoto T, Ono K (1996) Subaqueous eruption and emplacement of the Shinjima Pumice, Shinjima (Moeshima) Island, Kagoshima Bay, SW Japan. *J Volcanol Geotherm Res* 71:187–206

- Kato Y (1987) Woody pumice generated with submarine eruption. *Chishitsugaku Zasshi J Geol Soc Jpn* 93:11–20
- Kneller BC, Branney MJ (1995) Sustained high-density turbidity currents and the deposition of thick massive sands. *Sedimentology* 42: 607–616
- Kokelaar P, Raine P, Branney MJ (2007) Incursion of a large-volume, spatter-bearing pyroclastic density current into a caldera lake: Pavay Ark ignimbrite, Scafell caldera, England. *Bull Volcanol* 70:23–54. doi:10.1007/s00445-007-0118-5
- Komar PD (1971) Hydraulic jumps in turbidity currents. *Geol Soc Am Bull* 82:1477–1487. doi:10.1130/0016-7606(1971)82[1477:HJITC]2.0.CO;2
- Le Bas MJ, Le Maitre RW, Streckeisen A, Zanettin B (1986) A chemical classification of volcanic rocks based on the total alkali-silica diagram. *J Petrol* 27:745–750. doi:10.1093/petrology/27.3.745
- Lowe DR (1982) Sediment gravity flows: II. Depositional models with special reference to the deposits of high-density turbidity currents. *J Sediment Petrol* 52:279–297
- Manville V, Wilson CJN (2004) Vertical density currents: a review of their potential role in the deposition and interpretation of deep-sea ash layers. *J Geol Soc (London, UK)* 161:947–958. doi:10.1144/0016-764903-067
- Manville V, White JDL, Houghton BF, Wilson CJN (1998) The saturation behaviour of pumice and some sedimentological implications. *Sediment Geol* 119:5–16. doi:10.1016/S0037-0738(98)00057-8
- Manville V, Segsneider B, White JDL (2002) Hydrodynamic behaviour of Taupo 1800a pumice: implications for the sedimentology of remobilized pyroclasts. *Sedimentology* 49:955–976
- Matsumoto R, Katayama T, Iijima A (1985) Geology, igneous activity, and hydrothermal alteration in the Shimoda district, southern part of Izu Peninsula, central Japan. *J Geol Soc Jpn* 91:43–63
- McKee ED, Weir GW (1953) Terminology for stratification and cross stratification in sedimentary rocks. *Geol Soc Am Bull* 64:381–389
- McPhie J, Allen RL (2003) Submarine, silicic, syn-eruptive pyroclastic units in the Mount Read Volcanics, western Tasmania; influence of vent setting and proximity on lithofacies characteristics. In: White JDL, Smellie JL, Clague DA (eds) *Explosive subaqueous volcanism*. AGU, Washington, pp 245–258
- McPhie J, Doyle M, Allen R (1993) Volcanic textures. ARC - Centre of Excellence in Ore Deposits University of Tasmania, Hobart
- Mulder T, Alexander J (2001) The physical character of subaqueous sedimentary density flow and their deposits. *Sedimentology* 48: 269–299. doi:10.1046/j.1365-3091.2001.00360.x
- Piper DJW, Normark WR (2009) Processes that initiate turbidity currents and their influence on turbidites; a marine geology perspective. *J Sediment Res* 79:347–362. doi:10.2110/isr.2009.046
- Postma G, Nemeč W, Kleinspehn KL (1988) Large floating clasts in turbidites: a mechanism for their emplacement. *Sediment Geol* 58: 47–61
- Pyle DM (1989) The thickness, volume and grain size of tephra fall deposits. *Bull Volcanol* 51:1–15
- Raos AM, McPhie J (2003) The submarine record of a large-scale explosive eruption in the Vanuatu Arc; approximately 1 Ma Efate pumice formation. In: White JDL, Smellie JL, Clague DA (eds) *Explosive subaqueous volcanism*. AGU, Washington, pp 273–284
- Reynolds MA, Best JG, Johnson RW (1980) 1953–57 eruption of Tulumán Volcano; rhyolitic volcanic activity in the northern Bismarck Sea. Geological Survey of Papua New Guinea, Port Moresby
- Rivera J, Lastras G, Canals M, Acosta J, Arrese B, Hermida N, Micallef A, Tello O, Amblas D (2013) Construction of an oceanic island: insights from the El Hierro (Canary Islands) 2011–2012 submarine volcanic eruption. *Geology* 41:355–358
- Sawamura K, Sumi K, Ono K, Moritani T (1970) Geology of the Shimoda District; quadrangle series, scale 1:50,000, Tokyo (8) No. 105. Geological Survey of Japan
- Schneider JL, Le Ruyet A, Chanier F, Buret C, Ferrière J, Proust JN, Rosseel JB (2001) Primary or secondary distal volcanoclastic turbidities: how to make the distinction? An example from the Miocene of New Zealand (Mahia Peninsula, North Island). *Sediment Geol* 145: 1–22
- Shanmugam G (2002) Ten turbidite myths. *Earth Sci Rev* 58:311–341. doi:10.1016/S0012-8252(02)00065-X
- Shanmugam G (2008) Deep-water bottom currents and their deposits. In: Rebesco M, Camerlenghi A (eds) *Contourites*. Elsevier Science, Amsterdam, pp 59–81
- Sohn YK (1997) On traction-carpet sedimentation. *J Sediment Res* 67: 502–509
- Sohn YK, Chough SK (1993) The Udo tuff cone, Cheju Island, South Korea; transformation of pyroclastic fall into debris fall and grain flow on a steep volcanic cone slope. *Sedimentology* 40:769–786
- Stewart AL, McPhie J (2004) An Upper Pliocene coarse pumice breccia generated by a shallow submarine explosive eruption, Milos, Greece. *Bull Volcanol* 66:15–28
- Sumner EJ, Talling PJ, Amy LA, Wynn RB, Stevenson CJ, Frenz M (2012) Facies architecture of individual basin-plain turbidites: comparison with existing models and implications for flow processes. *Sedimentology* 59:1850–1887. doi:10.1111/j.1365-3091.2012.01329.x
- Sumner EJ, Peakall J, Parsons DR, Wynn RB, Darby SE, Dorrell RM, McPhail SD, Perrett J, Webb A, White D (2013) First direct measurements of hydraulic jumps in an active submarine density current. *Geophys Res Lett* 40:2013GL057862. doi:10.1002/2013GL057862
- Talling PJ, Amy LA, Wynn RB (2007) New insight into the evolution of large-volume turbidity currents: comparison of turbidite shape and previous modelling results. *Sedimentology* 54:737–769
- Talling PJ, Masson DG, Sumner EJ, Malgesini G (2012) Subaqueous sediment density flows: depositional processes and deposit types. *Sedimentology* 59:1937–2003. doi:10.1111/j.1365-3091.2012.01353.x
- Tamura Y (1990) Mode of emplacement and petrogenesis of volcanic rocks of the Shirahama Group, Izu Peninsula, Japan. Ph.D. thesis, University of Tokyo, Japan
- Tamura Y (1994) Genesis of island arc magmas by mantle-derived bimodal magmatism: evidence from the Shirahama Group, Japan. *J Petrol* 35:619–645. doi:10.1093/petrology/35.3.619
- Tamura Y (1995) Liquid lines of descent of island arc magmas and genesis of rhyolites: evidence from the Shirahama Group, Japan. *J Petrol* 36:417–434. doi:10.1093/petrology/36.2.417
- Tamura Y, Koyama M, Fiske RS (1991) Paleomagnetic evidence for hot pyroclastic debris flow in the shallow submarine Shirahama Group (Upper Miocene-Pliocene), Japan. *J Geophys Res* 96:21779–21787. doi:10.1029/91JB02258
- Tani K, Fiske RS, Tamura Y, Kido Y, Naka J, Shukuno H, Takeuchi R (2008) Sumisu volcano, Izu-Bonin arc, Japan: site of a silicic caldera-forming eruption from a small open-ocean island. *Bull Volcanol* 70:547–562
- Tani K, Fiske RS, Dunkely DJ, Ishizuka O, Oikawa T, Isobe I, Tatsumi Y (2011) The Izu Peninsula, Japan: Zircon geochronology reveals a record of intra-oceanic rear-arc magmatism in an accreted block of Izu-Bonin crust. *Earth Planet Sci Lett*. doi:10.1016/j.epsl.2010.12.052
- Taylor B (1992) Rifting and the volcanic-tectonic evolution of the Izu-Bonin-Mariana Arc. *Proc Ocean Drill Program Sci Results* 126: 627–652
- Valentine PC, Cooper RA, Uzzmann JR (1984) Submarine sand dunes and sedimentary environments in Oceanographer Canyon. *J Sediment Petrol* 54:704–715
- Watt SFL, Talling PJ, Vardy ME, Masson DG, Henstock TJ, Huehnerbach V, Minshull TA, Urlaub M, Lebas E, Le Friant A, Berndt C, Crutchley GJ, Karstens J (2012) Widespread and progressive seafloor-sediment failure following volcanic debris avalanche

- emplacement: landslide dynamics and timing offshore Montserrat, Lesser Antilles. *Mar Geol* 323–325:69–94
- White JDL (2000) Subaqueous eruption-fed density currents and their deposits. *Precambrian Res* 101:87–109. doi:[10.1016/S0301-9268\(99\)00096-0](https://doi.org/10.1016/S0301-9268(99)00096-0)
- White JDL, Manville V, Wilson CJN, Houghton BF, Riggs NR, Ort M (2001) Settling and deposition of AD 181 Taupo pumice in lacustrine and associated environments. In: White JDL, Riggs NR (eds) *Volcaniclastic sedimentation in lacustrine settings*. Blackwell Science, Oxford, pp 141–150
- White JDL, Smellie JL, Clague DA (2003) Introduction: a deductive outline and topical overview of subaqueous explosive volcanism. In: White JDL, Smellie JL, Clague DA (eds) *Explosive subaqueous volcanism*. AGU, Washington, pp 1–23
- Wright IC (1996) Volcaniclastic processes on modern submarine arc stratovolcanoes: sidescan and photographic evidence from the Rumble IV and V volcanoes, southern Kermadec Arc (SW Pacific). *Mar Geol* 136:21–39
- Wright IC (2001) In situ modification of modern submarine hyaloclastic/pyroclastic deposits by oceanic currents: an example from the southern Kermadec arc (SW Pacific). *Mar Geol* 172:287–307
- Wright IC, Gamble JA (1999) Southern Kermadec submarine caldera arc volcanoes (SW Pacific): caldera formation by effusive and pyroclastic eruption. *Mar Geol* 161:207–227
- Yamada E, Sakaguchi K (1987) Stratigraphy and geological structure of the Neogene formations, southwestern part of the Izu Peninsula, Japan. *Chishitsu Chosajo Geppo Bull Geol Surv Jpn* 38:357–383